TORSION OF EXTERIOR GIRDERS OF A STEEL GIRDER BRIDGE DURING CONCRETE DECK PLACEMENT LOADS: FIELD TEST REPORT

By
Thomas L. North
W. M. Kim Roddis

Structural Engineering and Engineering Materials
SL Report 99-1
March 1999

THE UNIVERSITY OF KANSAS CENTER FOR RESEARCH, INC.
2385 Irving Hill Drive - Campus West, Lawrence, Kansas 66044

Table of Contents

Table of Contents-continued

List of Figures

ABSTRACT

This report is the second part of a two part report. The first part is written and developed as a design aid to determine the torsion acting on outside steel bridge girders during concrete deck placement.

This second part reports results of measurements taken from two bridges. The first bridge is located at K-10 highway over I-70 between Lawrence and Topeka, Kansas. The second bridge is located on southbound I-635 highway over Swartz Road in Kansas City, Kansas.

During bridge construction, deck overhang loads occur on steel plate or rolled beam girders and are supported by cantilever brackets. In addition to supporting the weight of the placement screed, these brackets must also support the weight of the additional construction loads. The vertical loads applied on the deck are eccentric and generate large torsional moments at the intervals between cross bracing. The result of this loading effect is torsional moments that generate a combination of longitudinal stresses and loads from the cantilever brackets.

Strain gages were installed on the Swartz Road bridge to measure these overhang loads. A "Multiframe 4D" computer model was made to compare the results measured in the

field, with AISC recommendations, and with TAEG (Torsional Analysis of Exterior Girders) results.

The screed loads measured from the static load runs and analytical model were based on the locations of bogey and gang vibrators. In the analytical model, the loads were moved across the beam at quarter points beginning at midspan, then tabulated and plotted alongside the field results. After all of the moments representing the various load cases were compiled, an influence diagram was constructed from the loads measured in the field and the analytical model.

Loads were analyzed for two cases using the AISC method outlined in the "Design for Concrete Overhang Loads". The first load case represented the static field test while the second represented the results measured the day of concrete placement. The same wheel loading for the analytical model was used for the AISC calculations.

In some instances, the strains measured on the Swartz Road bridge were small. In these situations it can be difficult to guarantee the sensitivity and output of gage readings, however, the major axis moments measured on the Swartz Road bridge during static load testing were almost identical to the moments calculated with the Multiframe analysis. This shows that the loads that were used and how they were distributed in the Multiframe analysis were close to actual field conditions. This also shows consistent and accurate behavior of the strain gages.

No significant differences were found with the moments measured from the static load runs where blocking had been removed. More blocking had been provided than what was needed on the Swartz Road bridge, however, when concrete and live loads are added, the change in load response should be greater.

Surveying prisms were used to measure deflections during the load tests. The recorded and predicted maximum vertical deflections on the Swartz Road bridge were consistently close for all load runs. Horizontal deflections were not observed at any location.

The Multiframe model used to calculate torsional bending did match closely with the moments measured in the field at midpoint between stiffeners but varied greatly between measured and analytical results for endpoint locations. The computer model used to calculate torsional bending did not match as closely with the moments measured in the field. The difference between measured and analytical results varied for maximum values but was in relative agreement for the trends of the moments. Most of the differences can be attributed to the lateral stiffness provided by a combination of deck formwork and a portion of concrete deck in place in the Northbound lanes. Unfortunately, the loose play of the formwork connections to the girder makes the lateral stiffness difficult to measure.

Some of the differences in the torsional moments that were calculated using the Multiframe model and the TAEG program can be attributed to some basic model assumptions. The Multiframe analysis was based on a non-prismatic girder section that

was continuous over diaphragm locations. The TAEG program assumes a three span, prismatic member.

A comparison of torsional moments calculated by TAEG show a large difference in results from field measurements, the torsional model, and AISC calculations. In some cases the differences are small and in others they are significant. For the static field tests and the Multiframe torsion models, the trends show close similarity, however the maximum loads for all locations do vary. The TAEG program was always conservative in comparison to the field results and the multiframe model. Since the TAEG program is intended to be used as an in-house design aid, this conservative approach is regarded as positive.

INTRODUCTION

1.1 General

Concrete is distributed and finished on a bridge deck using a placement screed (see figure 1). This screed moves back and forth, from abutment to abutment, on two rails mounted on the deck overhangs. During bridge construction, deck overhang loads that occur on steel plate or rolled beam girders are usually supported by cantilever brackets placed every three to four feet (see figure 2). In addition to supporting the weight of the placement screed, these brackets must also support the weight of the construction workers, the formwork, and the plastic concrete.

The vertical loads applied on the deck overhangs are transferred to the outside fascia girders. These loads are eccentric and generate large torsional moments at the intervals between cross frames that act as lateral bracing. The concrete placement loads tend to twist the top flange of the girder outward. The result of this loading effect are torsional moments that generate longitudinal stresses combined with resultant loads in the cantilever brackets having the potential to cause significant lateral deflections.

In isolated instances, the torsional deflections of the exterior girders have resulted in insufficient cover on top reinforcing steel and concrete leakage through deck formwork [AASHTO, 1996].

1.2 Motivation

Prior to this research project, the Kansas Department of Transportation used an in-house computer spreadsheet to predict the torsional response of construction loads on steel beam bridges [KDOT, 1997]. This spreadsheet is based on the criteria outlined in the AISC publication "Design for Concrete Deck Overhang Loads" [AISC, 1990]. However, due to the lack of information on loading and torsional restraint, the spreadsheet output is considered approximate in determining actual torsional behavior. This discrepancy between design assumptions and actual conditions can lead to diaphragm bracing situations that are either over or under designed.

1.3 Object and Scope

This report is the second part of a two part report. The first part is written and developed as a design aid to determine the torsion acting on outside steel bridge girders during concrete deck placement [Roddis, 1997]. In addition to the design aid, an example has been provided that represents conditions on the Swartz Road bridge the day of deck placement.

This second part reports the results of measurements taken from two bridges. The first bridge is located at K-10 highway over I-70 between Lawrence and Topeka, Kansas [Roddis, 1995], (See Appendix A). The second bridge is located on southbound I-635 highway over Swartz Road in Kansas City, Kansas.

The K-10 bridge was tested in October, 1995, with the intent to measure deflections and strains due to normal concrete finishing operations. Appendix A outlines the general site and weather conditions, testing procedures, equipment used, and problems that occurred on the day of testing. Appendix A also explains performance of testing techniques and recommends improvements for future testing.

This report is a follow up on the recommendations outlined in the K-10 bridge report given in Appendix A. It describes the field testing performed on the Swartz Road bridge in October, 1996, to measure deflections and strains during deck placement. This report outlines the site and weather conditions, the testing procedures and equipment used on the day of testing. This report also discusses the current construction practices and typical overhang deck load conditions found on Kansas bridges. In addition, an analytic model has been used to compare the results measured in the field with both AISC recommendations and with TAEG (Torsional Analysis of Exterior Girders). Some of the past experiences with problems associated with concrete deck placement on bridges are discussed and recommended practices to improve the cost effectiveness and performance of deck overhang formwork are outlined.

This report is the final part of the project KTRAN # KU-96-3, MATC-KU-95-2, "Torsion of Exterior Girders of a Steel Girder Bridge During Concrete Deck Placement". The purpose of this project is to provide information on the response of torsional loads that occur on outside steel girders during concrete deck placement. This information will be used to help develop a consistent and accurate design aid for determining the required diaphragm bracing on outside girders for bridges in the state of Kansas.

1.4 Introduction

The existing southbound I-635 bridge over Swartz Road was constructed in 1979 (see figure 3). The original bridge was a three span, 172 foot, 34 inch deep, non-prismatic, welded steel plate girder structure with a roadway width of 51 feet along a skew of 32° 23' 24". In October, 1996, the original deck of the structure was removed, the east column bents extended, an additional rolled beam girder added, and the roadway widened to 58 feet (see figure 4).

Although there was heavy traffic volume along the Swartz Road bridge, no interruptions of traffic or construction occurred during testing.

1.5 Description of Methods

For the Swartz Road bridge, three different instruments were used to measure strains, deflections and forces:

1. Strain Gauges on Steel Beams

   Strain Gauges were attached at various locations on the bridge to measure the fascia girder strains (see figure 5 for locations).

2. E.D.M. (Electronic Distance Measurement) Prisms

A total of four magnetically mounted surveying prisms were placed on the steel plate girders to measure vertical, horizontal and torsional deflections of fascia girders (see figure 6 for locations).

3. Strain Gage Load Cell

A calibrated load cell was used to measure compressive forces in the lower flange blocking of the outside fascia girder during concrete deck placement (see figure 4 for location).

The strain gauges were placed Tuesday, October 15, through Thursday, October 17, 1996. On Friday, October 18, all gauges were wired and all switch boxes were tested. Static load tests were run on Monday, October 24 and final load tests were run on the day of concrete deck placement, Tuesday, October 25.

1.6 Load Conditions

A 40 foot Gomaco, C-450 concrete finisher was used as a static load to test the structural response of the I-635 bridge. The finisher was mounted parallel to the centerline of the bridge and rode on 2-two inch diameter pipe rails mounted on opposite sides. With operator and fuel, the maximum load placed along the west edge of the bridge deck overhang was approximately 5346 lbs.

In comparison, the static load used to test the K-10 bridge was a 48 foot Bidwell Truss Finisher. The total dead load riding along one side of the bridge deck overhang was approximately 12,202 lbs.

The deck replacement of the southbound I-635 bridge was done in two phases. Phase one involved 22 feet of deck removed from the East Side. An additional rolled beam girder, shear studs, and new reinforcing was added and the new deck placed. Phase two involved the removal of the remaining 31 feet of concrete deck followed by new shear studs, reinforcing, and concrete.

For most bridges, a concrete deck is normally placed by a screed mounted on rails that overhang on both sides. In contrast, the Gomaco finisher was riding on overhang brackets on the West Side of the southbound I-635 bridge. The other side of the finisher was riding on rails mounted on the west edge of the new concrete deck. In addition to dead and live loads imposed by equipment and personnel during the deck placement, one lane of traffic was being carried on the East Side of the bridge.

The Swartz Road bridge had 4 x 4 timbers used as lateral blocking. These were placed midway on each diaphragm on the exterior bay, between girders A and B only (see figure 4). The diaphragms measured 18 inches deep and were steel bent plates welded to the web stiffeners. There are two diaphragms in the outside spans and three in the center span of the bridge. The timber blocking was placed just above the bottom flanges (see figure 7).

Nine static load passes were made on the bridge by the Gomaco screed. The strain was measured on the load cell and girder strain gauges from each pass and recorded. In addition, load deflections were measured and recorded using magnetic E.D.M. prisms. Quarter points were marked on the west fascia girder and were used to indicate the screed position. These quarter points were labeled from "0" at the south abutment to "6" in the middle of the bridge. At every point where measurements were taken, the screed was centered over the chosen quarter point. The test results are tabulated in Appendix D.

Prior to the first static load pass, the screed made several load passes back and forth on the bridge to seat the strain gages mounted on the girder, work out any slippage in the bolted connections and check for repeatability of strain measurements. With the exception of run # 9, all load runs were started on the second quarter point in span two. For load run # 9, the load was started from the first quarter point in span two. The static screed load was moved from quarter points 1 through 6 and measurements were recorded. In the first, second and third passes, all lateral blocking was kept in place while loads were placed at quarter points and measurements taken. In the fourth and fifth passes, all lateral blocking was removed in the first span except for one timber left in the middle of the center bay. The loads were placed along quarter points and measurements taken. In the sixth, seventh and eighth passes, all lateral blocking was removed in the first span and the static screed load placed from quarter points 1 through 7. For pass # 9, the day of concrete placement, all lateral blocking was in place. The strains that were measured were from a combination of concrete, finisher, and workmen.

1.7 Formwork

The formwork on the I-635 bridge was typical of most bridges constructed in Kansas. The exterior girder formwork started with overhang brackets spaced at about four foot centers (see figures 7 & 7a). These were attached directly to diagonal lagstuds and then to tieback hangers. Bearing transverse and on top of the brackets were double 2 x 4s. On top of these and parallel to the outside girder were 4 x 4 timbers. On top of the 4 x 4 timbers, a deck of 3/4 inch plywood was nailed and a 2 x 4 lumber railing provided. The formwork for the concrete guardrail was located 2.47 feet from the centerline of the outside girder and was directly on top of the plywood deck. The formwork for the guardrail was approximately four foot tall and was comprised of 3/4 inch plywood nailed to 2 x 4s at 24 inch centers. The screed rail was located directly on top of the guardrail formwork and had steel whalers attached at about six foot centers.

For the interior formwork, double 2 x 10 lumber was placed transverse at about six foot centers. These 2 x 10s were hung from the top flange using a tieback hanger. The tieback hanger is a 1/2 inch diameter threaded steel rod with oversized washers and plates on the top and bottom and holds the double 2 x 10 beam in place. The 2 x 10s were bearing directly against the inside face and along the top of each girder. On top of the double 2 x 10s were 4 x 4 inch timbers placed parallel to the bridge and spaced at about 16 inch centers. On top of the 4 x 4 timbers, a deck of 3/4 inch plywood was nailed, followed by two layers of reinforcement.

1.8 Weather Conditions

Eight inches of snow had fallen in the Kansas City area two days before the day of testing. All gages had been attached and protected prior to the snowfall. The static load tests for the Swartz Road bridge began at 11:00 am, Monday, October 24, 1996, and continued until 5:30 p.m. the same evening. The weather for most of the day was partly cloudy with temperatures ranging between 65° F and 68° F. The next day when the concrete deck was placed, the skies were cloudy with temperatures holding a steady 48° F. Trucks began delivery of concrete about 9:00 am and continued until shortly after 1:00 p.m.

1.9 Strain Gauges

For the Swartz Road bridge, a total of twelve linear strain gauges were attached. (see figure 5). The three locations, marked A, B and C, were placed in the middle of the center diaphragm bay, in alignment with a diaphragm and toward the end of span one. The gage placed at location A was used to determine beam behavior at either side of a bearing point. The gage at location B was placed to determine load behavior and boundary conditions at a diaphragm. The gage at location C was used to measure load behavior in the middle of a diaphragm span.

All gauges were attached according to manufacturer recommendations and were the type CEA-06-250UW-120. These were chosen because they were easier to attach and performed as well as the EA-06-250BG-120 gages used previously on the K-10 bridge [Doyle,1989]. Four strain gages were used at each location and were located 3/8 inch from the outside edges of the top and bottom flanges. The top gages were mounted on the bottom of the top flange. The bottom gages were mounted on the top of the bottom flange. After the gauges were attached, each was tested for 120 ohm resistance and given an environmental protective coating of Teflon tape, RTV sealant and a butyl rubber coating. All of the leadwires were given a protective coat of waterproof heat-shrink and

RTV sealant. All of the cable used was Belden M 8723 fully shielded 4-wire type with a length of 75 feet.

The readout and switching units for the strain gauges were wired and tested for complete circuits and voltage fluctuations. All of the strain readouts measured in the field were consistent throughout each load pass.

1.10 Load Cell

The load cell transducer used on the Swartz Road bridge was machined from a 1/2" dia. 6061 aluminum stock [Hannah, 1992]. The load cell had four, EA-06-250BG-120 foil strain gauges attached, two in the transverse direction and two in the lateral direction. All of the gages were wired as a full bridge to insure reasonable averaging of load eccentricity and to amplify the axial strain signal. For initial calibration, the load cell was loaded in the laboratory at 1000 pound increments to a maximum of 5000 pounds. Strain vs. load curves were plotted and a regression analysis performed prior to installation to insure linear behavior. Afterwards, the load cell was given a protective coating of Dow 3145 RTV sealant and placed in a PVC shield prior to installation in the field.

The load cell was attached to the end of the lateral blocking timber at location C. A threaded collar had been fitted that would allow the load cell to be adjusted by hand and tight against the web. No initial strain measurements had been taken to measure the compression acting on the web prior to loading.

1.11 Surveying Prisms

A request was made to the Kansas Department of Transportation, district one office in Topeka, to send a survey crew with a total station system to the bridge site. Using an EDM, they measured horizontal and vertical deflections from the magnetic swivel head reflectors mounted on the bridge girder.

The magnetic reflectors were placed at four locations on the bridge (see figure 6). A reference angle was shot from a benchmark to a point on top of the south pier. The reflector heads were mounted on swivels that could be adjusted to point perpendicular to the EDM. This helped to eliminate errors that might result from extreme angle shots.

A Wild T-1000 theodolite with an error of three seconds (plus or minus 1/32-inch at a distance of 200 feet) was used to translate distances and elevations into x, y, and z coordinates.

2.0 Field Results

After the strain results were tabulated, each of the four strain values were graphed on a spreadsheet based on bridge location. From these values, the separate component for major axis bending was calculated using the relationship:

$$\varepsilon_{Major} = 1/2 \, (TL + TR)$$

$$\varepsilon_{Major} = -1/2 \, (BL + BR)$$

Where:

ε_{Major} = Major axis strain (μin/in)

TL = Top left of beam cross section

TR = Top right of beam cross section

BL = Bottom left of beam cross section

BR = Bottom right of beam cross section

Torsional strain was calculated based on the assumption that the lateral stiffness on the Swartz Road bridge was significant enough that no minor axis bending was occurring in the girders. This assumption was verified by measurements taken in the field for lateral displacement. Because of this, whatever strain remained after major axis bending was calculated represented lateral strain in the top or bottom flange and could be translated into torsion bending. In addition, because of the lateral resistance provided by the deck formwork, the girder tended to rotate about the top flange. Strain gage readings show a greater amount of bending on the bottom flange in comparison to the top. After major axis strain was calculated, torsional strain was determined by taking the measured values of strain and then subtracting the major axis strain. This method was used for all locations and yielded the result:

$$\varepsilon_{Torsion} = \varepsilon_{Total} - \varepsilon_{Major}$$

The method for deriving moments from recorded strains is illustrated in Appendix B [Willems, 1981].

2.1 AISC Recommendations

The AISC publication "Design for Concrete Deck Overhang Loads", 1990, outlines an approximate method for determining factored positive and negative moments based on an equivalent fixed end beam analogy [AISC, 1990]. The assumption is made that the bridge diaphragms, or cross frames, act as torsionally rigid supports that prevent out of plane warping [Salmon, 1996]. The deck overhang loads are resisted by equal and opposite

lateral forces acting at the cantilever brackets. These are located along the outside girder on the top and bottom flanges. The lateral bending stiffness of the web is considered negligible.

In effect, each flange acts as a laterally loaded fixed end beam with a span equal to the distance between each cross frame [AISC, 1983]. From this model, both the total maximum lateral moments due to lateral forces acting on the equivalent fixed end beam and maximum normal flange stresses can be computed.

The flanges are then checked against permanent deformations and ultimate strength. Two tables have been provided in the AISC guide to check for stress in the top and bottom girder flanges. These tables assist in computing the maximum moment in the middle and at the end of each cross frame based on overhang distances, girder depths and diaphragm spacing.

2.2 Analytic Results

A separate computer model for major axis bending and torsional bending was assembled using the structural analysis package "Multiframe 4D" (see figure 8). Each of the test passes made in the field was represented by a static model with a corresponding load condition. These models were used to predict the load response behavior of the outside bridge beam. Each computer model was constructed based on span, varying section properties and load conditions [Young, 1989]. In the field, the loads were placed across

the skew. However, the finishing rail and wheel lines were parallel to the bridge with the overhang brackets perpendicular to the girder. Because of this perpendicular load arrangement, no provisions were needed for the effects of skew.

The loads that were included for the computer model of the static screed test (see figure 9), prior to concrete placement, were screed loads and live loads. The screed loads were based on information obtained from the contractor and from the technical staff representing the Gomaco Corporation in Ida Grove, Iowa.

Screed Loads	
Basic weight	4200 lbs
2 - 8 foot extensions	1050 lbs
EPD Package	300 lbs
Fuel	12 lbs
Operator	200 lbs
Subtotal assembly weight	5762 lbs

In addition to the screed assembly loads, the moving loads are as follows:

Gang vibrators	600 lbs
Rack	300 lbs
Upper Carriage	900 lbs
Lower carriage	800 lbs

The total loads represented compute to a concentrated load of 5346 lbs. For the flexural analysis, this load is distributed evenly between four wheels, representing a wheel load of

1337 lbs. For the torsional analysis, the concentrated load is distributed between three overhang brackets at four foot spacing.

The dead loads used for the analysis of actual deck placement (see figure 10) included screed loads, two roller assemblies used by finishers and concrete. The live loads that were used represented one operator, an assistant and a finisher on each end of the screed. In addition, finishers were also placed on both ends of the two roller assemblies behind the screed while three finishers were placed within the tributary width of the outside beam. The deadload of the structure, formwork and rebar loads were not included in either analysis. These loads were in place when the strain gages were attached.

The location and distribution of screed loads was based on the operation of the carriage assembly and gang vibrators during concrete deck placement. The fresh concrete is pumped to a carriage assembly, or bogey. As the concrete is pumped, the bogey moves back and forth, distributing the concrete across the deck. At the same time, a series of concrete vibrators move back and forth across the deck in the same manner and in the opposite direction. Because the bogey and the gang vibrator assembly move back and forth and in opposite directions along the bridge deck, they cross at some point. It is this point (see figure 9, "Deck Placement Loads") at which the two assemblies cross that creates the largest concentrated load along a concrete placement screed. This crossing point most often occurs somewhere in the middle of the bridge deck, but because the bogey and gang vibrators run independently of each other, the highest load concentration

can sometimes occur at the outside edge of the steel girder. It is this load condition that represents the greatest screed load on the brackets supported by the outside girder.

The screed loads used for the static load runs, along with the analytical model, was based on the location of both bogey and gang vibrators at the very end of the screed. This represented the greatest torsional load the outside girder would experience. However, during actual concrete placement, the screed would have to be stopped and started several times to repeat this same load pattern. To model the load pattern for run # 9, the middle crossing point was used for the bogey and gang vibrator location.

The load responses measured from each model was compiled and tabulated into a spreadsheet from Microsoft Excel for ease of processing and comparison. A continuous line chart was used to define the data points representing moment response. No information is available from Microsoft regarding the specific mathematical method used to curve fit through the data points. After all of the moments representing the various load cases were compiled, an influence diagram was constructed based on the static loads measured in the field from the three strain gage locations [Pilkey, 1994].

The Multiframe computer model representing major axis bending was assembled using distributed and concentrated wheel loads acting on top of the outside bridge beam. The model consists of a continuous beam with pinned supports on the ends and roller supports at the piers (see figure 8). In a manner similar to the field tests, the loads in the major axis

bending model were moved across the beam at quarter points beginning at midspan. The moments were then tabulated and plotted alongside the field results (see figure 11).

The computer model for torsional bending was based on the AISC analogy of a top and bottom girder flange acting independent of the web and as a laterally loaded beam. The AISC model consists of fixed end points and spring supports at the diaphragm locations. In contrast, the Multiframe torsional analysis consists of a continuous beam with diaphragms represented by pinned supports. No provision had been made for the added stiffness of the upper deck formwork or by lateral blocking. The loads on the torsional analysis begin at midspan and are moved across the beam at quarter points in the same manner as the original static field loads. The moments were then tabulated and plotted alongside the field results (see figure 12).

The lateral loading was based on an 8'-7" wheel line pattern on the screed. Two load distributions were considered. The first load pattern was evenly distributed along three cantilever brackets and comprised of three concentrated loads of 1.782 kips, spaced at four foot intervals. In the field, these cantilever brackets transfer the wheel loads to the lower flange and are distributed as three concentrated loads acting parallel along the major axis of the flange. The second load pattern was based on the distribution of the 8'-7" wheel line through four feet of plywood formwork. The total load was distributed at a 45 degree angle to a total length of 16.583 feet with .284 kips/ft acting along the lower flange.

The section modulus varied on the existing girder at different locations. Location A was at a point 10 inches north of the bearing device between spans 1 and 2. At this point, the stiffness of the girder is significantly increased due to the fixity of the top and bottom flanges, the deck formwork and a bearing device. In addition, stiffeners are located in the middle and in close proximity of both sides of the bearing device. The strain gages for location B were attached along a four inch web stiffener that connected a bent plate diaphragm. The strain gages at location C were attached on the girder away from any web stiffeners and between two diaphragms.

2.3 Comparison

The results for major axis and torsional bending from the distributed and concentrated load models were virtually the same. Because of this, all of the results shown in this report (with the exception of the test data from the actual deck placement) are based on a concentrated load model represented by run # 6. For run # 9, the loads that were used were a combination of concentrated loads for the screed and roller assemblies and distributed loads for live and fresh concrete.

For run # 6, the Multiframe model used to calculate major axis bending was within general agreement of the maximum moment measured in the field for all locations (see figure 11). After comparing the differences between measured and analytical results, an almost identical value for minimum and maximum moments occur within the first span of the bridge. The major differences between the two results begin to appear towards the

middle of the bridge. In span one, location A, the maximum moment measured in the field was 26.9 k-ft while the calculated maximum moment was 22.6 k-ft. For location B, the maximum moment measured in the field was 32.6 k-ft while the calculated maximum moment was 21.9 k-ft. For location C, the maximum moment measured in the field was 32.0 k-ft while the calculated maximum moment was 39.3 k-ft.

At all locations on the girder, the measured moments in the bottom flange were larger than the moments in the top. On the quarter point 23.5 feet from the abutment, run # 6, the measured moment at location A in the bottom flange exceeds that of the top flange by a factor of 28, at location B by a factor of 1.6, and at location C by a factor of 2.9.

The Multiframe model used to calculate torsional bending did not match as closely with the moments measured in the field (see figure 12). The difference between measured and analytical results did vary for maximum values but was in relative agreement for the trends of the moments. In span one, location A, the maximum lateral moment measured in the field was 2.6 k-ft while the calculated maximum lateral moment was 1.5 k-ft. For location B, the maximum lateral moment measured in the field was 5.4 k-ft while the calculated maximum lateral moment was 13.8 k-ft. For location C, the maximum lateral moment measured in the field was 2.5 k-ft while the calculated maximum lateral moment was 3.5 k-ft.

For the deck placement, run # 9, the Multiframe model used to calculate major axis bending was in general agreement of the maximum moment measured in the field for

location C (see figure 13), however locations A and B show some disagreements in both maximum values and trends. In span one, location A, the maximum moment measured in the field was 381.1 k-ft while the calculated maximum moment was 296 k-ft. For location B, the maximum moment measured in the field was 216.2 k-ft while the calculated maximum moment was 175.8 k-ft. For location C, the maximum moment measured in the field was 130.4 k-ft while the calculated maximum moment was 127.8 k-ft.

The Multiframe model used to calculate torsional bending did match closely with the moments measured in the field at location C (see figure 14). But again, the difference between measured and analytical results for locations A and B did vary for maximum moments and their trends. In span one, location A, the maximum lateral moment measured in the field was 21.7 k-ft while the calculated maximum lateral moment was 1.2 k-ft. For location B, the maximum lateral moment measured in the field was 4.0 k-ft while the calculated maximum lateral moment was 22.6 k-ft. For location C, the maximum lateral moment measured in the field was 2.3 k-ft while the calculated maximum lateral moment was 6.8 k-ft. The maximum lateral moments occurring anywhere in span one are 21.7 k-ft measured at A and 22.6 k-ft measured at B. Much better agreement was found for maximum moment magnitude rather than location.

Loads were then analyzed for two conditions using the AISC method outlined in the "Design for Concrete Overhang Loads", (see Appendix 3). The first load condition represented the static field test conducted the day of October 21st. The second method represented testing that had taken place the day of concrete placement. The same wheel

loading for the analytical model was used for the AISC calculations. To calculate the actual stresses, the factor for noncomposite dead load (1.3) was omitted.

Using the AISC method for run # 6, the static field test, the value calculated for fixed end negative moment was 11.5 k-ft. At location B, the maximum negative moment measured in the field was 5.4 k-ft while the maximum negative moment calculated from the Multiframe torsional model was 13.8 k-ft. Using the AISC method, the value of the maximum positive moment in between cross frames was calculated to be 6.9 k-ft. The maximum positive moment measured in the field was 2.5 k-ft and the maximum positive moment calculated from the torsional model was 3.5 k-ft.

Using the AISC method for run # 9, the concrete deck placement run, the value calculated for negative fixed end moment in the flange at location B was 22.6 k-ft. The maximum negative moment measured in the field was 4.0 k-ft while the maximum negative moment calculated from the Multiframe torsional model was 22.6 k-ft. From the AISC method, the value of the maximum positive moment in between cross frames was calculated to be 12.8 k-ft.

The maximum positive moment measured in the field was 2.3k-ft and the maximum positive moment calculated from the Multiframe torsional model was 6.6 k-ft.

From these values, the ratio of continuous beam, pinned end to mid-span moments range from 0.25 to 0.58. The value for fixed end to mid-span moment used by AISC to

calculate mid-span moments is 0.53. The calculated fixed end to mid-span moments from the TAEG example of the Swartz Road Bridge, with and without timber blocking, is 0.93.

A comparison of torsional moments calculated by TAEG show a large difference in results from field measurements, the torsional model, and AISC calculations. TAEG shows the value for fixed end moment in the flange at location B to be 62.7 k-ft, [Roddis,1997]. The maximum moment measured in the field was 4.0 k-ft, the Multiframe torsional model was 22.6 k-ft, and using the AISC method, 22.6 k-ft. TAEG shows the value for the maximum moment in between cross frames to be 58.2 k-ft. The maximum moment measured in the field was 2.3 k-ft, from the torsional model, 6.6 k-ft, and from AISC calculations, 12.8 k-ft.

An additional comparison was made for the effects of blocking during static load runs # 3, # 4, and # 6 in the first span. Load run # 3 had all blocking in place, load run # 4 had one blocking timber left in the middle of span one, and load run # 6 had all blocking removed in the first span.

In most cases, the data did show a trend that would indicate a larger increase in load based on the subsequent removal of timber blocking. However, in some cases the data showed either very little difference or a decrease in load (see table 1). For major axis bending (see figures 15 through 17), location A showed a change of 24.4, 29.6 and 24.4 k-ft for load runs # 3, # 4, and # 6 respectively. Location B measured a change of 25.3, 24.4, and 29.6 k-ft for load runs # 3, # 4, and # 6, while at location C, a change of 25.7,

27.8, and 28.3 k-ft during load runs # 3, # 4, and # 6 were measured. For torsional bending (see figures 18 through 20), location A showed a change of 3.0, 3.3 and 3.3 k-ft for load runs # 3, # 4, and # 6 respectively. Location B measured a change of 5.7, 4.9, and 5.4 k-ft for load runs # 3, # 4, and # 6, while at location C, a change of 2.2, 2.1, and 2.5 k-ft during load runs # 3, # 4, and # 6 were measured.

The loads to the blocking timber at location C (see figure 21) measured by the load cell vary as much as 70 pounds between runs # 3 and # 4. This was partly due to an inherent, unmeasurable amount of slip in the formwork and bracket connections. The maximum strain measurements showed that the blocking at location C experienced greater loads during runs # 2 and # 3 than at runs # 4 and #5 (an average of 280 lbs. and 93 lbs. respectively) while run # 9 showed a maximum load of 433 lbs.

The maximum vertical deflections recorded at prism A was + 0.12 inches (see figure 22). This occurred during the period the screed was in the second span and was consistently the same for all load runs. The predicted deflection at this point was + .003 inches. No vertical deflections were recorded at prism B, although predicted deflections were almost identical to location A. The recorded and predicted maximum vertical deflections at prism C was - 0.12 inches. This occurred during the time the screed was in the first span and was consistently the same for all load runs. Horizontal deflections were not observed at any location.

2.4 Discussion

The primary intent of the first test of the K-10 bridge was to gain an appreciation for existing field conditions, determine appropriate instrumentation and refine environmental protection systems. The measurements taken at the Swartz Road bridge implements those improvements learned from the results of the K-10 bridge.

In some instances, the strains measured on the Swartz Road bridge were small. In these situations it can be difficult to guarantee the sensitivity and output of strain gage readings, however, the major axis moments measured on the Swartz Road bridge during static load testing were almost identical to the moments calculated with the Multiframe analysis. This implies that the loads that were used and how they were distributed in the Multiframe analysis were close to actual field conditions. This also shows consistent and accurate behavior of the strain gages.

In some instances, the differences between the torsional moments measured in the field and the results obtained with the Multiframe analysis varies substantially. These differences are attributed to the lateral stiffness provided by the deck formwork. The design of bridge deck formwork is similar throughout the country, however, differences do occur with formwork connections to the girder and the amount of loose play they

exhibit. The varied results of the center diaphragm load cell confirms this. This variable can be difficult, if not impossible to measure.

Some of the differences in the torsional moments that were calculated using the Multiframe model and the TAEG program can be attributed to some basic model assumptions. The Multiframe analysis was based on a non-prismatic girder section that was continuous over diaphragm locations. The diaphragms are welded to the girders in a fashion that would allow some rotation to occur. These locations are represented as pinned supports and are spaced along the entire bridge length. The area of the Swartz Road bridge that was measured and analyzed was in the first span. The first span is 47 foot long and has a diaphragm spacing of 17.01 ft., 18.15 ft., and 11.84 ft. The negative maximum end moments in the middle diaphragm spacing was located at a very stiff girder section (I_x = 426.7 in^4). The maximum positive moment in the middle diaphragm spacing was located at a much smaller girder section (I_x = 60.8 in^4). The loads that used were based on finishing screed, concrete, and construction workers. The deadload of the structure, formwork and rebar loads were not included in either the Multiframe or AISC analysis.

In contrast, the TAEG analysis is based on a 47 foot span with fixed end boundary conditions. The girders were considered prismatic and were assigned a moment of inertia of 426.7 in^4 throughout. The diaphragms were equally spaced and represented as spring supports. In addition to the finisher, concrete and live loads that were used, a formwork

deadload of 13.4 psf was included. A portion of the Northbound lanes also had a new concrete deck. This provided torsional resistance that TAEG is unable to duplicate.

The results from the TAEG program were always conservative in comparison to the field results and the Multiframe model. Since the TAEG program is intended to be used as a design aid, this conservative result is regarded as positive.

2.5 Summary of Observations

For the K-10 bridge, the readouts of the strain gages showed excessive amounts of scatter and spiking due to the wet weather. For the static load testing on the Swartz Road bridge, small amounts of scatter were measured on the strain gauge readouts but overall, were consistent. The manufacturers' recommendations for application and environmental protection were closely followed. The combinations of Teflon tape, RTV sealant and a butyl rubber coating provided good protection against the humidity and heavy snow that occurred prior to testing.

During actual deck placement, the strain gauges again were consistent, however, some problems did occur with radio frequency interference from the concrete trucks. This interference was observed as short, excessive spikes on the readout dials and was discarded as reliable data.

For the K-10 bridge, the magnetically mounted surveying prisms were the most convenient and reliable method for measuring deflections and rotations. Unfortunately, the Swartz Road bridge not only had half of a new deck already in place but was also a considerably stiffer structure. Because of this, the outside girder of the Swartz Road bridge did not experience any horizontal deflections, although the small vertical deflections that were measured during the various load passes were consistent, reliable, and had a predictable amount of instrument error.

No significant differences were found with the moments measured from the static load runs where blocking had been removed. More blocking had been provided than what was needed on the Swartz Road bridge, however, when concrete and live loads are added, the change in load response should be greater. This is due to the fact that the Swartz Road bridge overhang was on one side only. The benefit of blocking and tierods is obtained when a continuous compression loadpath is provided from one overhang to a balancing overhang on the other side of the bridge.

There are differences between the moments measured in the field, those analyzed by the Multiframe model, and those calculated from the TAEG program (see table 2). In some cases the differences are small and in others they are significant. For the static field tests and the Multiframe torsion models, the trends show close similarity, however the maximum loads for locations A, B, and C differ by a magnitude of 1.24, 2.56, and 1.36 respectively.

For the deck placement run, locations B and C differ by a magnitude of 5.6 and 2.8 respectively. The difference in moments calculated by the TAEG program and the results from the Multiframe analysis for locations B and C differ by a magnitude of 2.8 and 8.8 respectively. The test results did show good agreement with the analytic model for maximum lateral moment magnitude, although location of that moment disagreed strongly.

At all girder locations, the strains measured in the bottom flange exceeded those in the top. In contrast, the stress results calculated by TAEG show the reverse. This is due to the stiff, in-plane loaded concrete deck on the Southbound Swartz Road bridge. The presence of the new deck reduced the top flange stress which could not be modeled in TAEG.

2.6 Recommendations

The ratio of fixed end to mid-span moment used by AISC (0.53) appears to be conservative when compared to the measured ratio of continuous beam, pinned end to mid-span moment (0.25 to 0.58). The measured values do show a large degree of variance. Until a more accurate method is developed, the AISC ratio should remain in use.

The fixed end negative moments calculated using the AISC load tables are in general agreement with the Multiframe torsional model, however, both appear conservative when compared to the moments measured in the field. Depending on the location, the deck

formwork may increase the resistance to torsion by as much as 130 % to 260 %. After previewing the comparisons in blocking and the force applied to the load cell, the lagstud and tieback hanger connections are experiencing a considerable amount of play. A loadpath cannot be followed on this plywood decking with any certainty until this play is eliminated.

The greatest concern for any state DOT is the issue of public safety. There is a considerable difference in results between the various methods of analysis that are outlined in this report. Of the methods that are described, the TAEG program was always conservative when compared to the field test results, the AISC analysis, and the multiframe model. Since the TAEG program is intended to be used as an in-house design aid, this conservative result is regarded as positive.

REFERENCES

AASHTO, "Standard Specifications for Highway Bridges", 16th Ed., 1996

AISC Marketing Inc., "Design for Concrete Deck Overhang Loads", 1990

AISC Marketing Inc., "Torsional Analysis of Steel Members", 1983

Doyle, James F., Phillips, James W., " Manual on Experimental Stress Analysis", 5th Ed., 1989

Hannah, R.L., Reed, S.E., " Strain Gage Users Handbook", 1992

Kansas Department of Transportation- Bridge Department, " Design Manual, Bridge Section - Metric", Vol. 3, 1997

Pilkey, Walter D., "Formulas for Stress, Strain, and Structural Matrices", 1994

Roddis, W. M. Kim, Kriesten, Mark, "Torsion of a Steel Girder Bridge During Concrete Placement - A design Aid", 1997

Roddis, W.M. Kim, North, Thomas L., " Field Testing of K-10 Bridge over I-70", 1995, (Enclosed as Appendix A)

Salmon, Charles G., Johnson, John E., " Steel Structures: Design and Behavior", 4th Ed., 1996

Willems, Nicholas, Easley, John T., Rolfe, Stanley T., " Strength of Materials", 1981

Young, Warren C., "Roarke's Formulas for Stress and Strain", 6th Ed., 1989

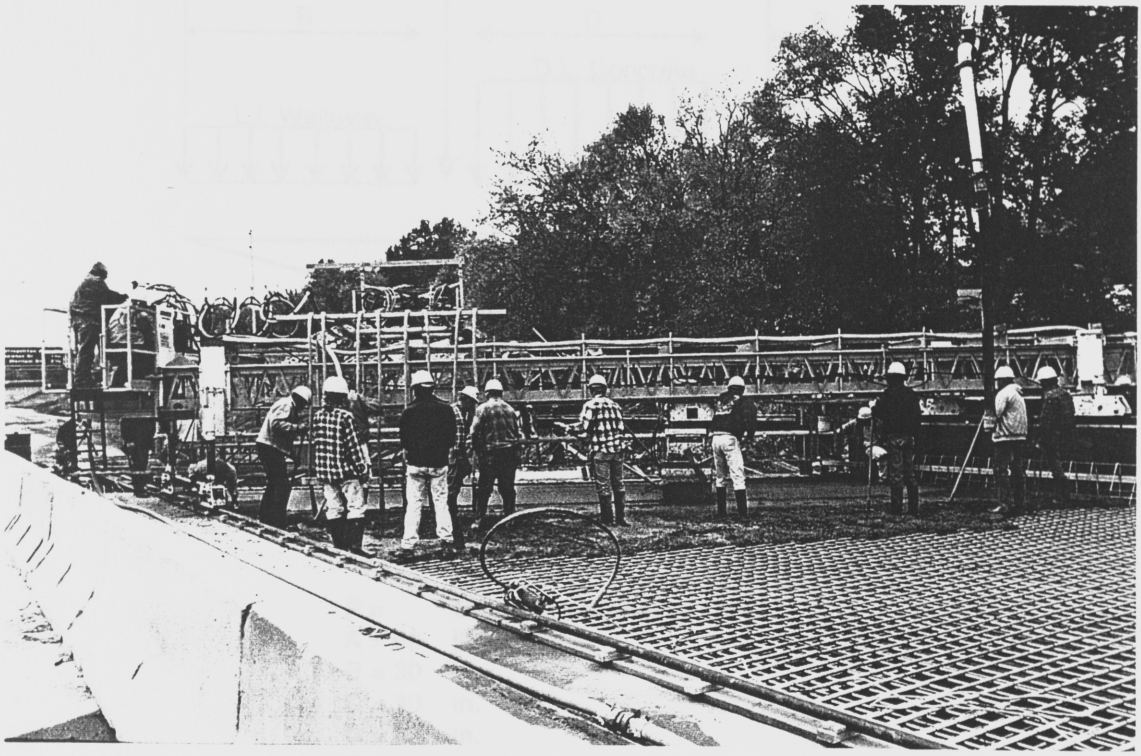

Figure 1 - Typical Screed

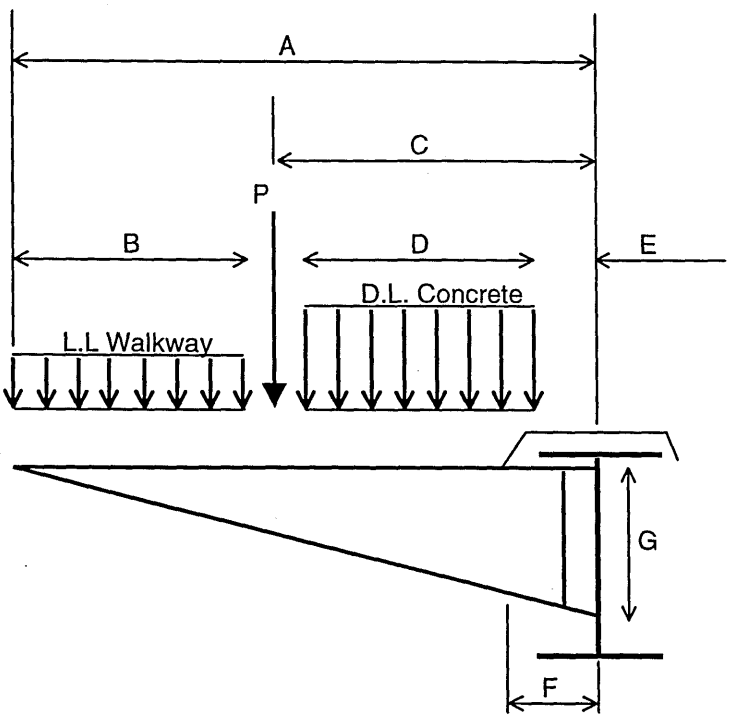

Bracket Dimensions and Loads

P =	**Maximum Wheel Load**
A = 60	**in.**
B = 30	**in.**
C = 30	**in.**
D = 22	**in.**
E = 8	**in.**
***F = 18**	**in.**
G = 30	**in.**

***Note: Estimated**

Figure 2 - Bracket Dimensions & Loads for Run # 9

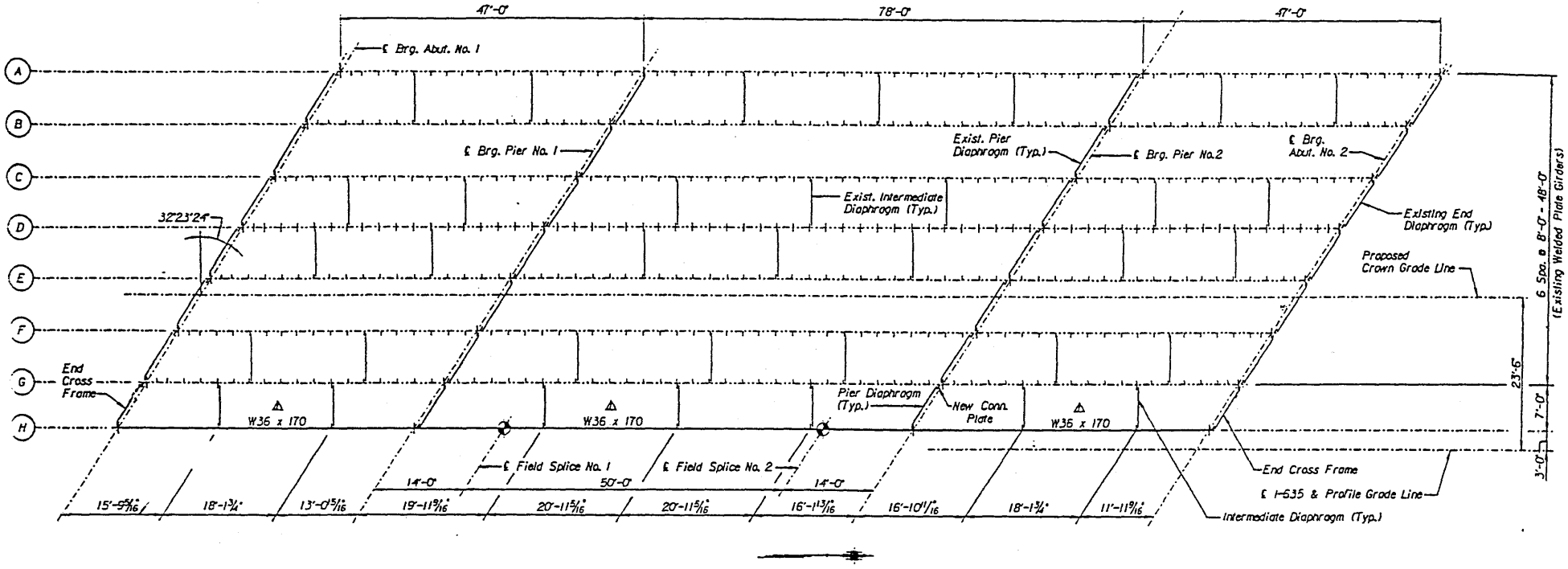

Figure 3 - Framing Plan, Southbound I-635 Bridge
(Courtesy of the Kansas Dept. of Transportation)

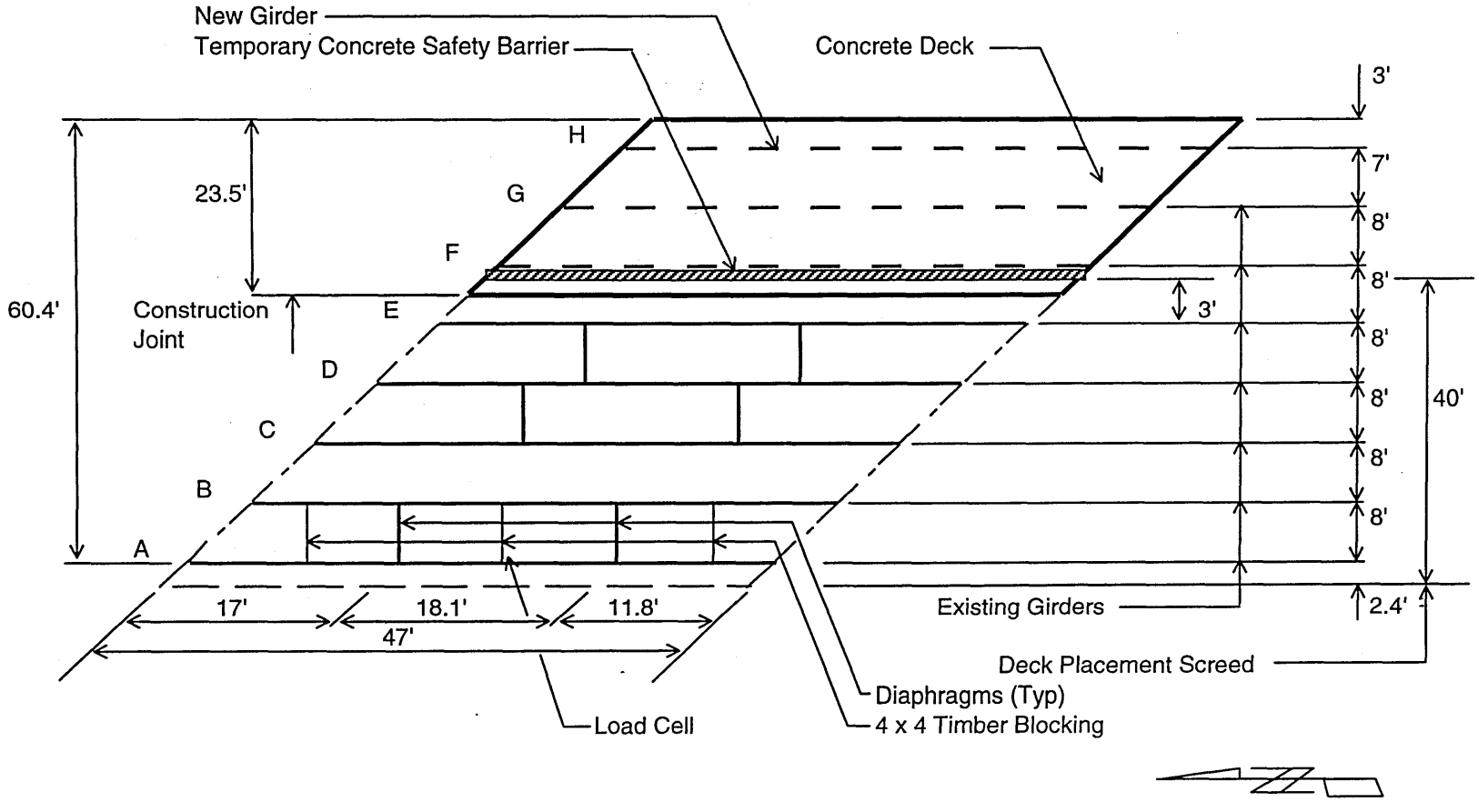

Fig. 4, Plan View, Span 1, Southbound I-635 Bridge

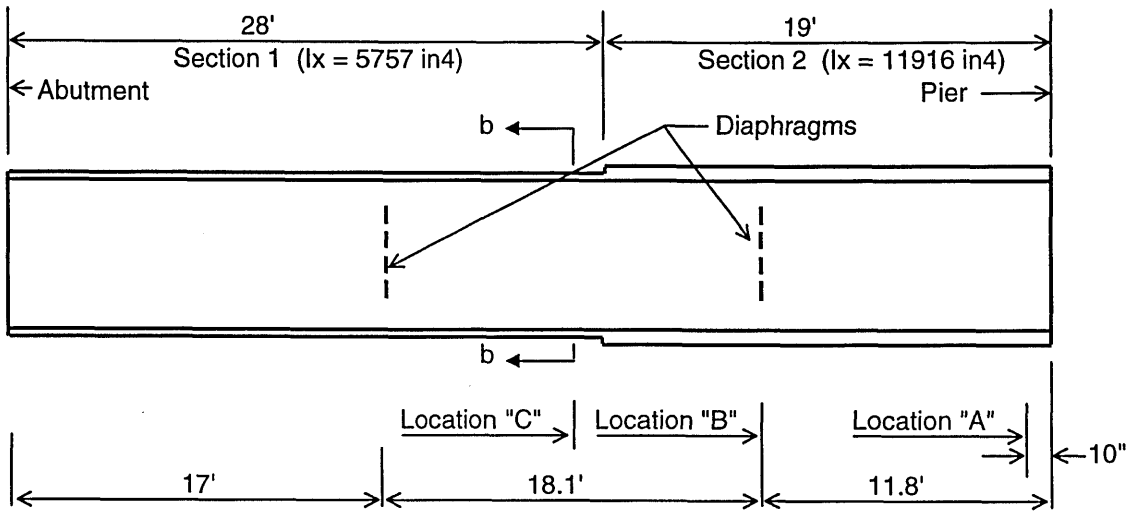

Span 1

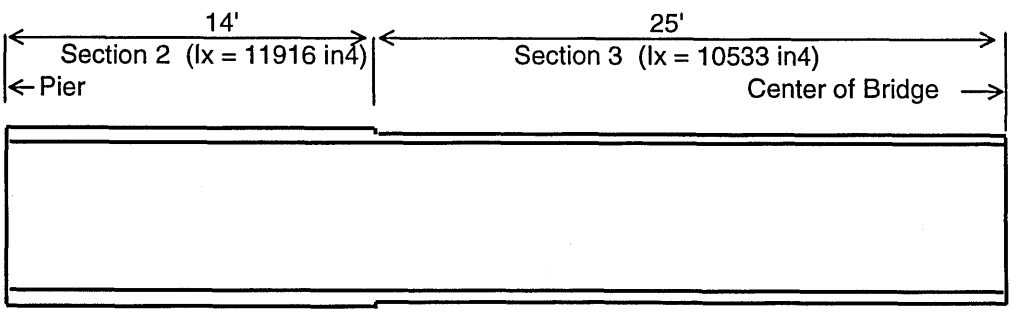

Span 2

Section A - A

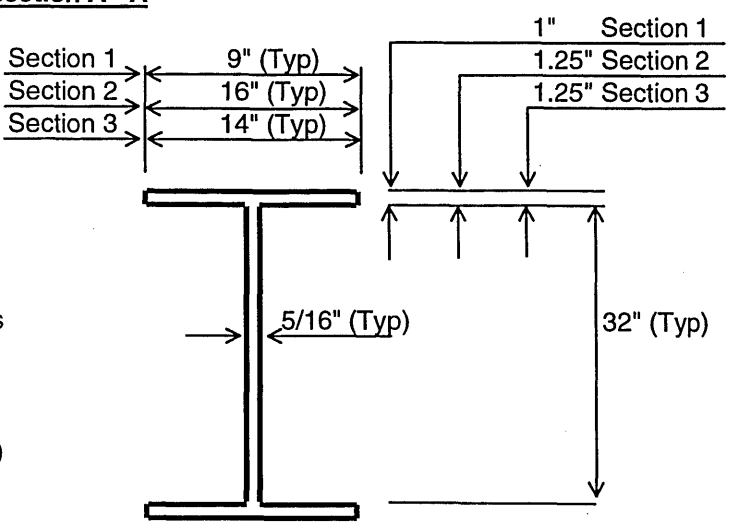

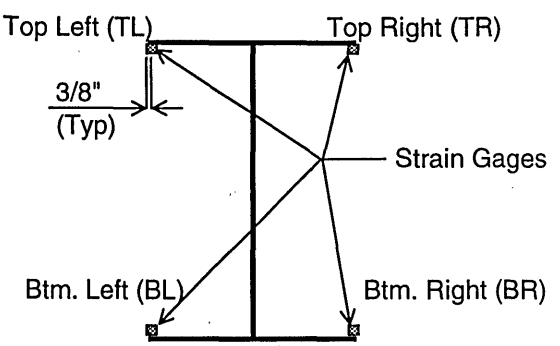

Section b - b, Strain Gage Locations

Beam Cross Sections

Figure 5 - Strain Gage Locations

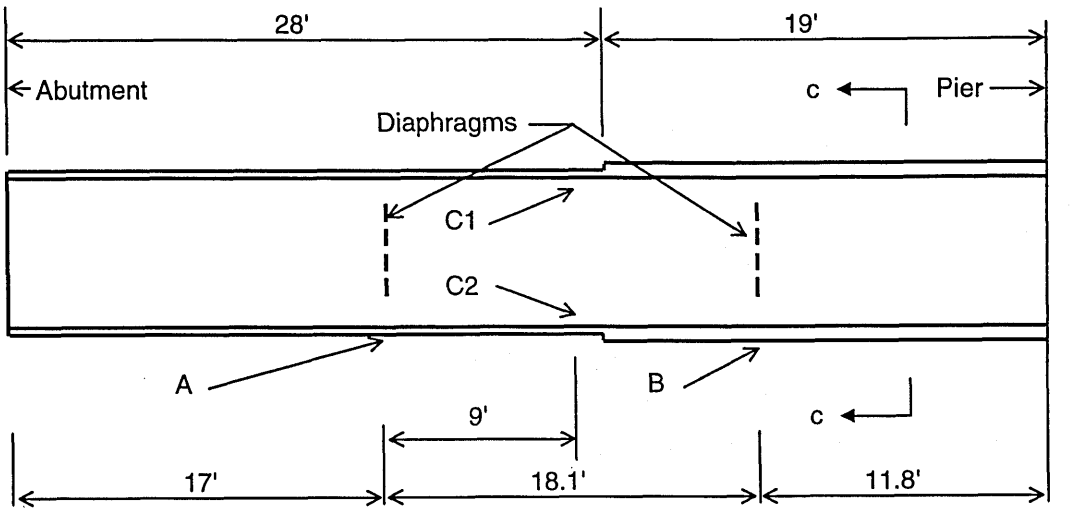

Span 1

Prism Locations

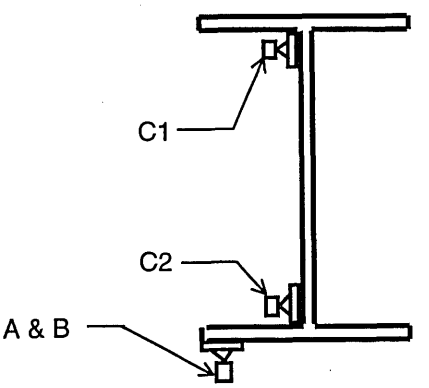

Section c - c, Prism Locations

Figure 6 - Prism Locations

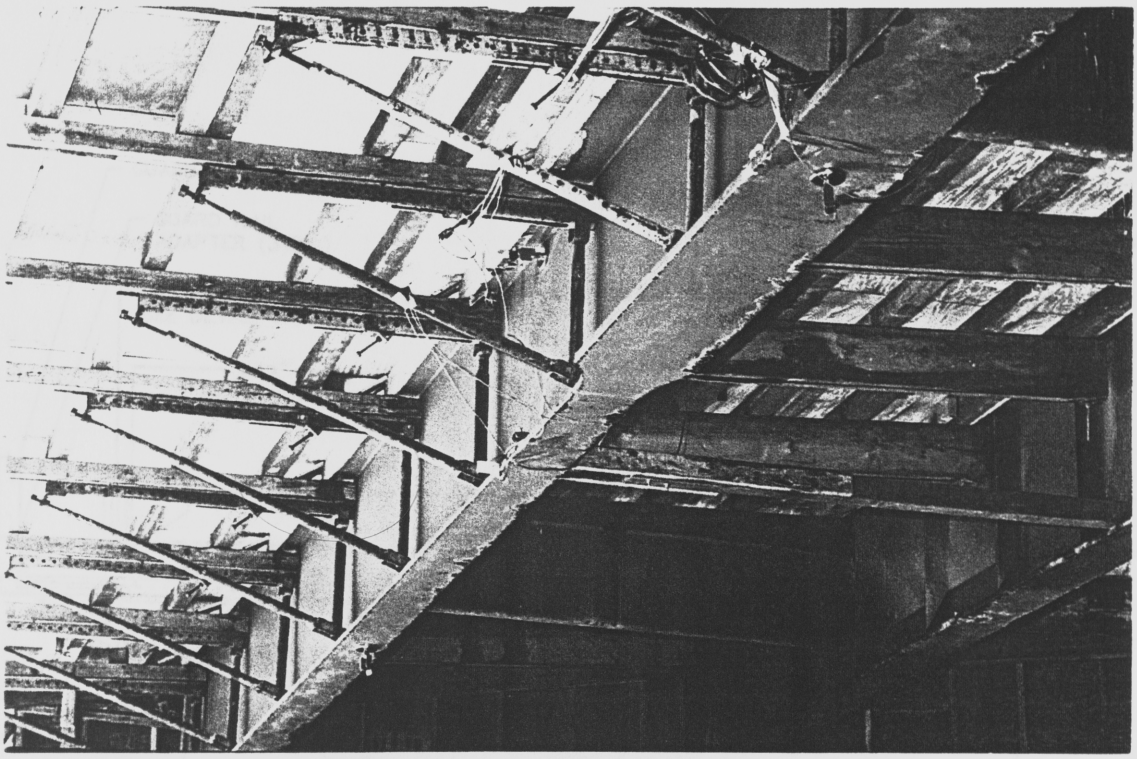

Figure 7 - Overhang Formwork

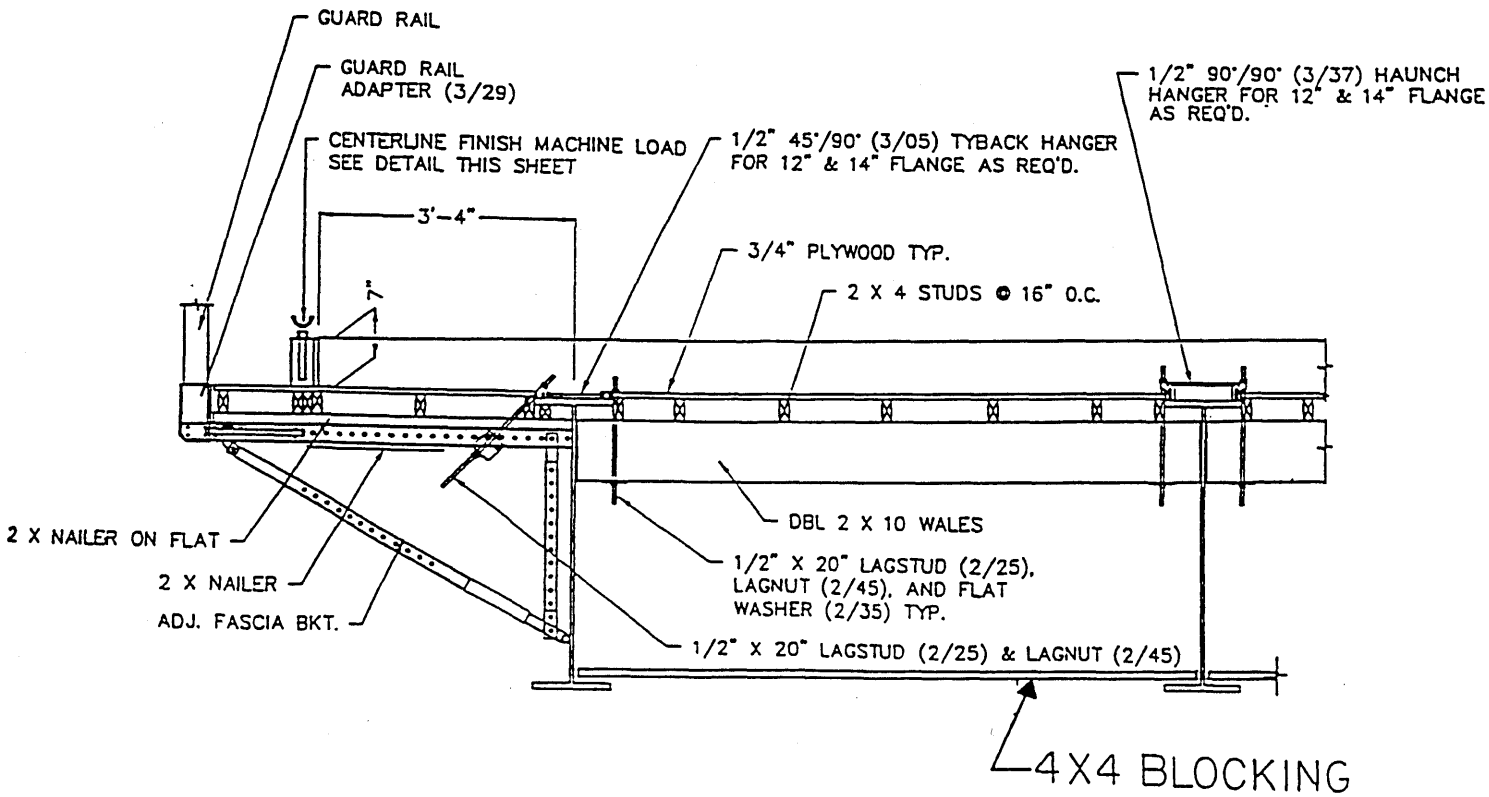

Figure 7A - Overhang Formwork-Layout

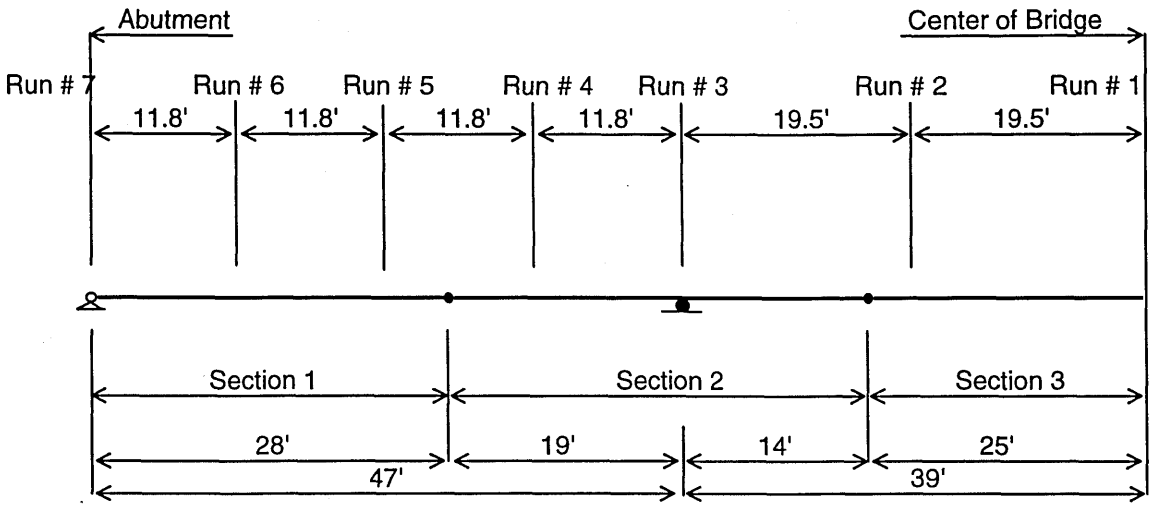

Support Conditions - Flexural Model Showing Quarter Point Locations

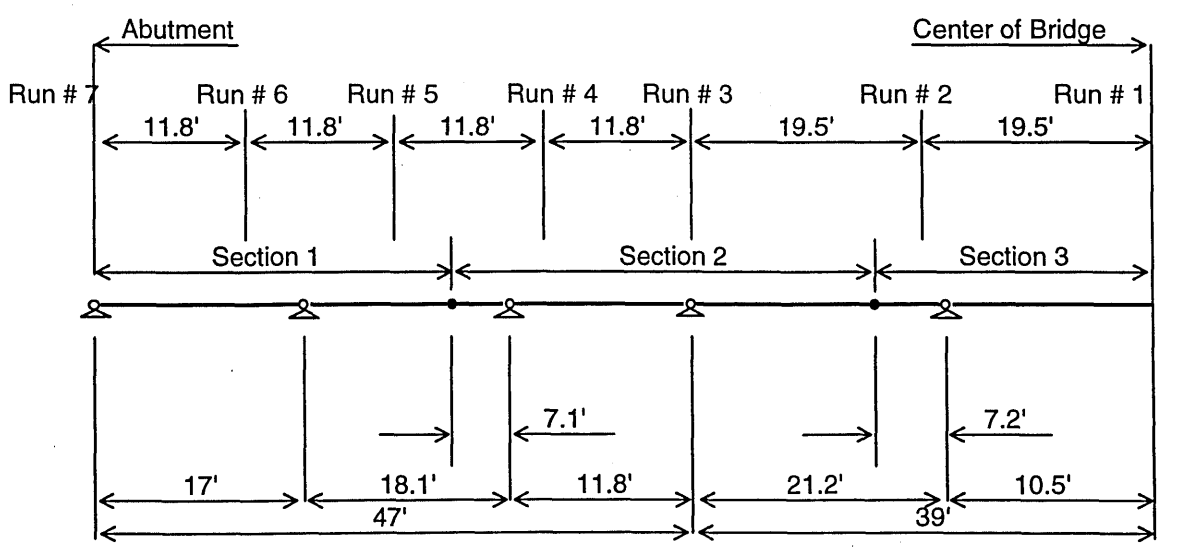

Support Conditions - Torsional Model Showing Quarter Point Locations

Figure 8 - Multiframe Analysis

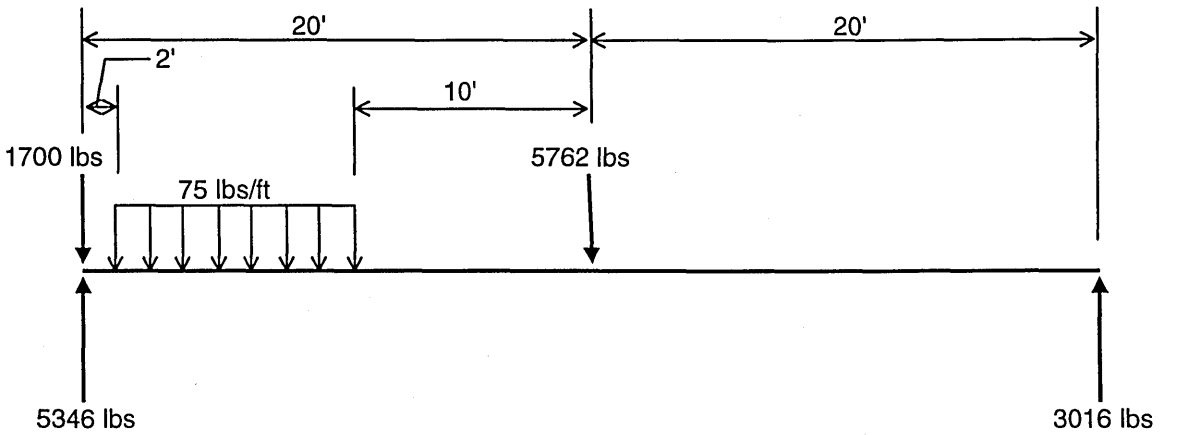

Screed Loads - Runs # 1 thru # 8

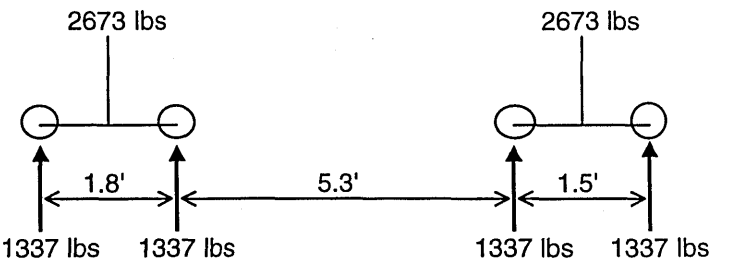

Wheel Loads - Runs # 1 thru # 8

Static Field Loads

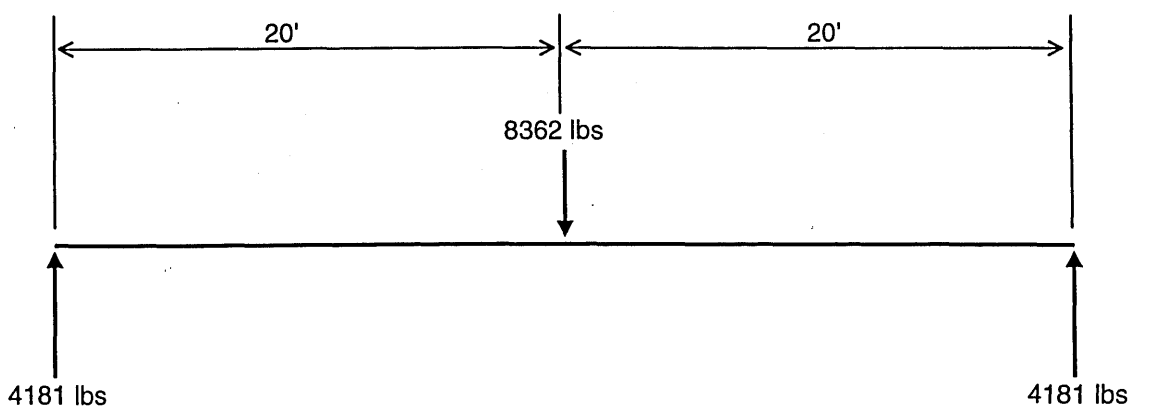

Deck Placement Loads

Figure 9 - Screed Loads

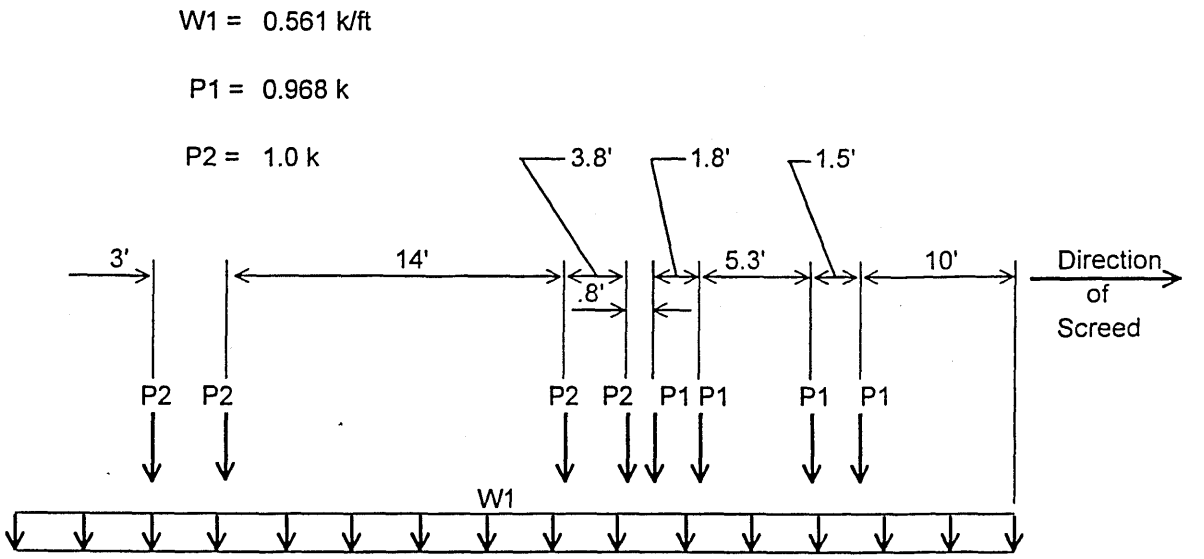

FLEXURAL LOADS

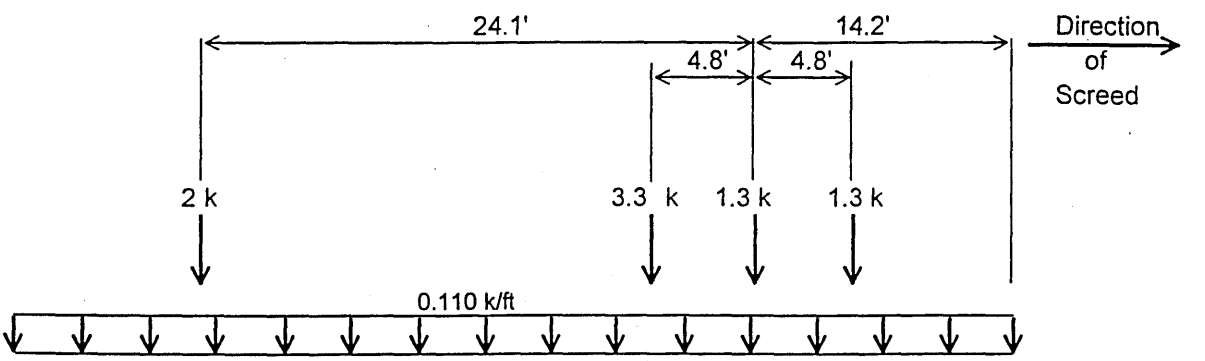

TORSIONAL LOADS

Figure 10 - Flexural & Torsional Loads for Run # 9

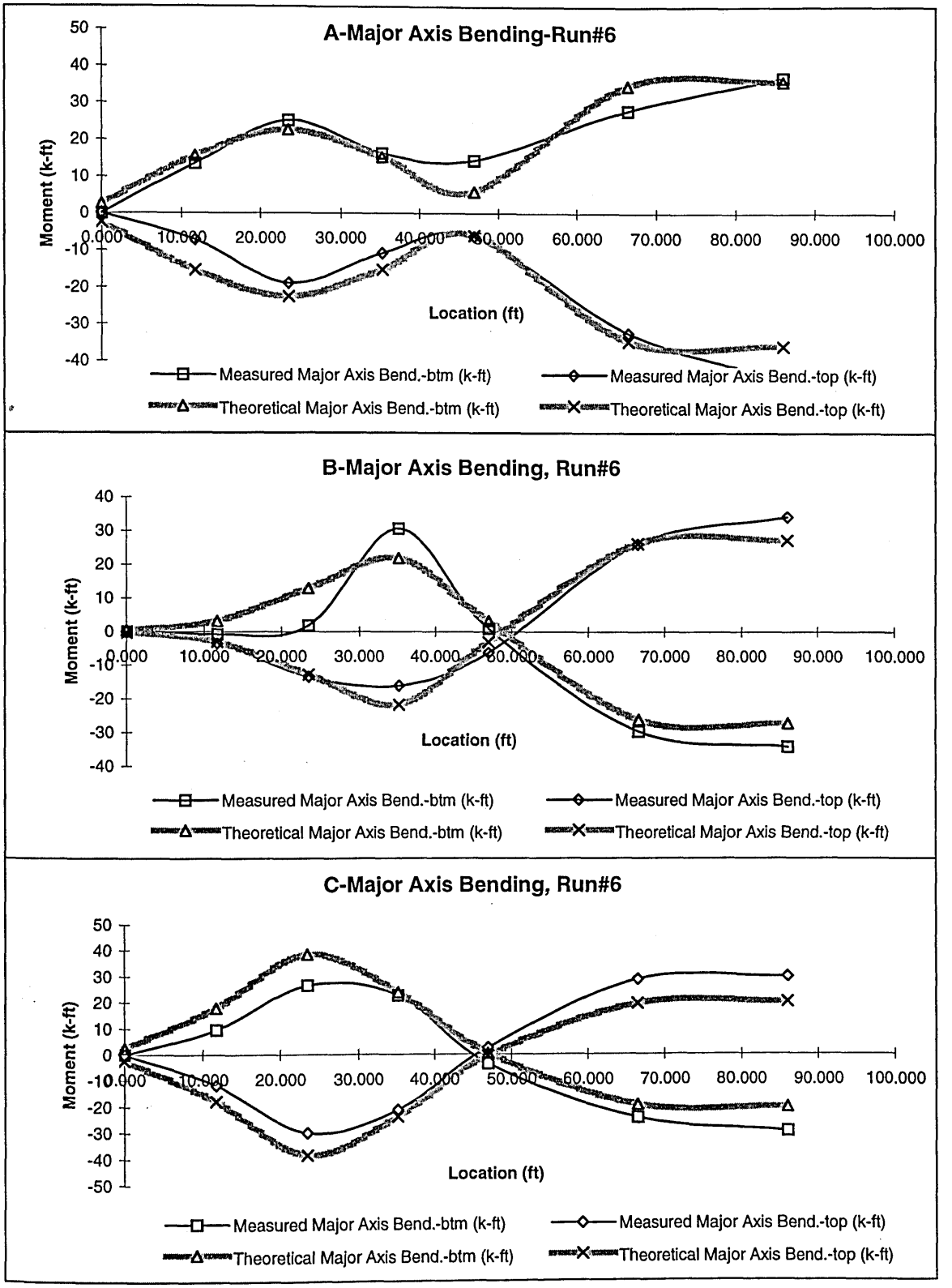

Figure 11 -Static Run Results, Major Axis Bending

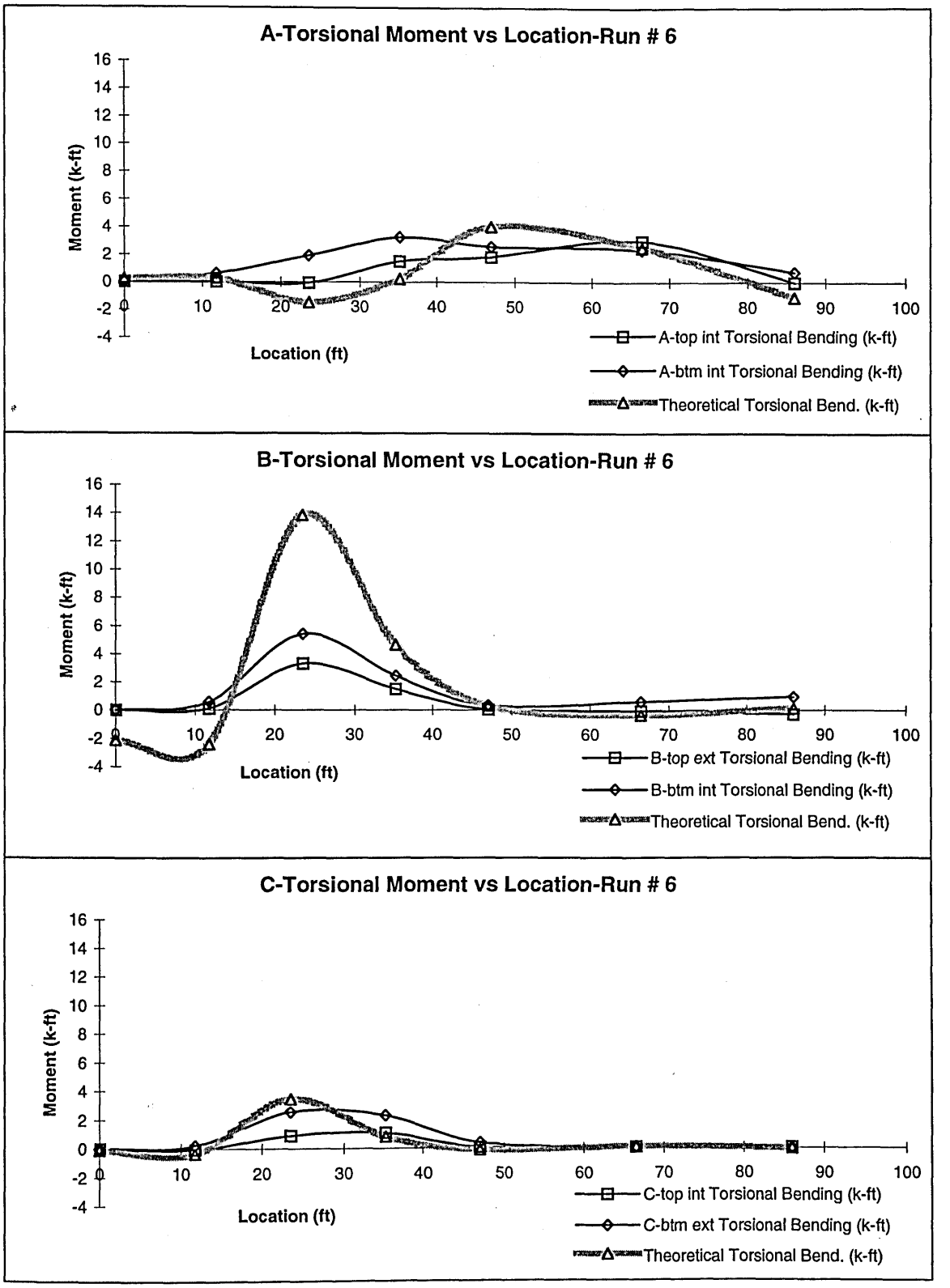

Figure 12 - Static Run Results, Torsional Bending

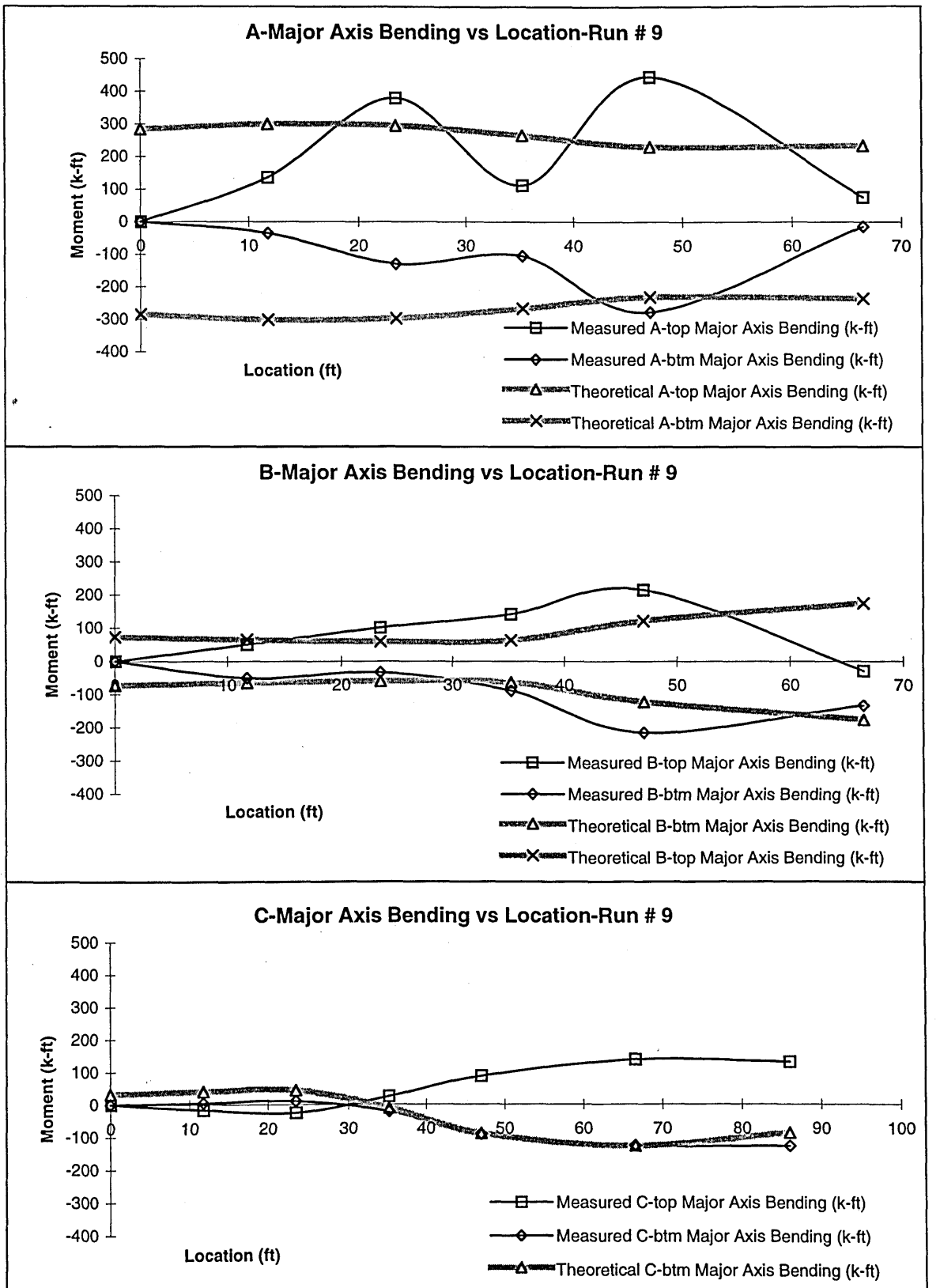

Figure 13 - Concrete Placement, Major Axis Bending

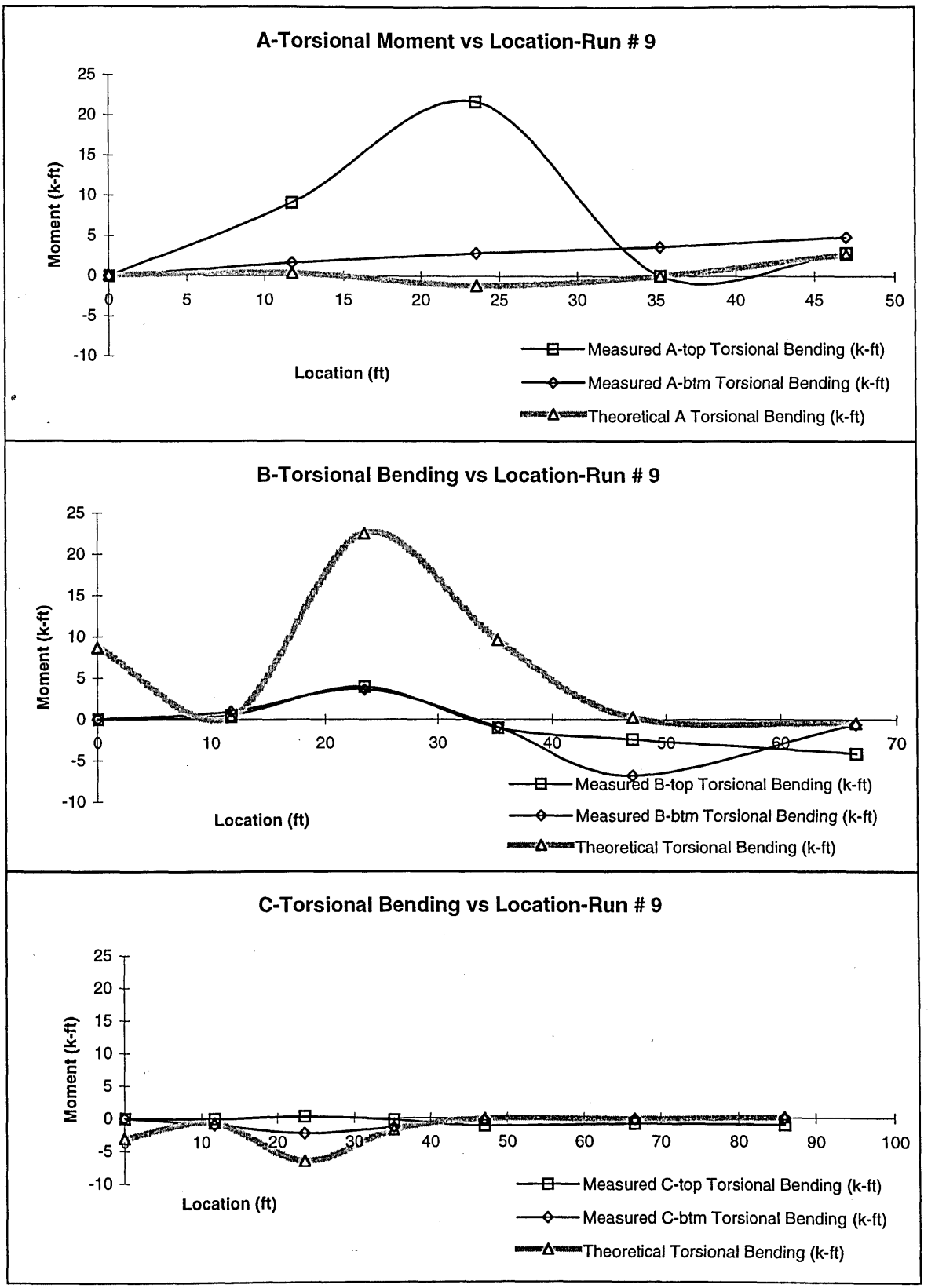

Figure 14 - Concrete Placement, Torsional Bending

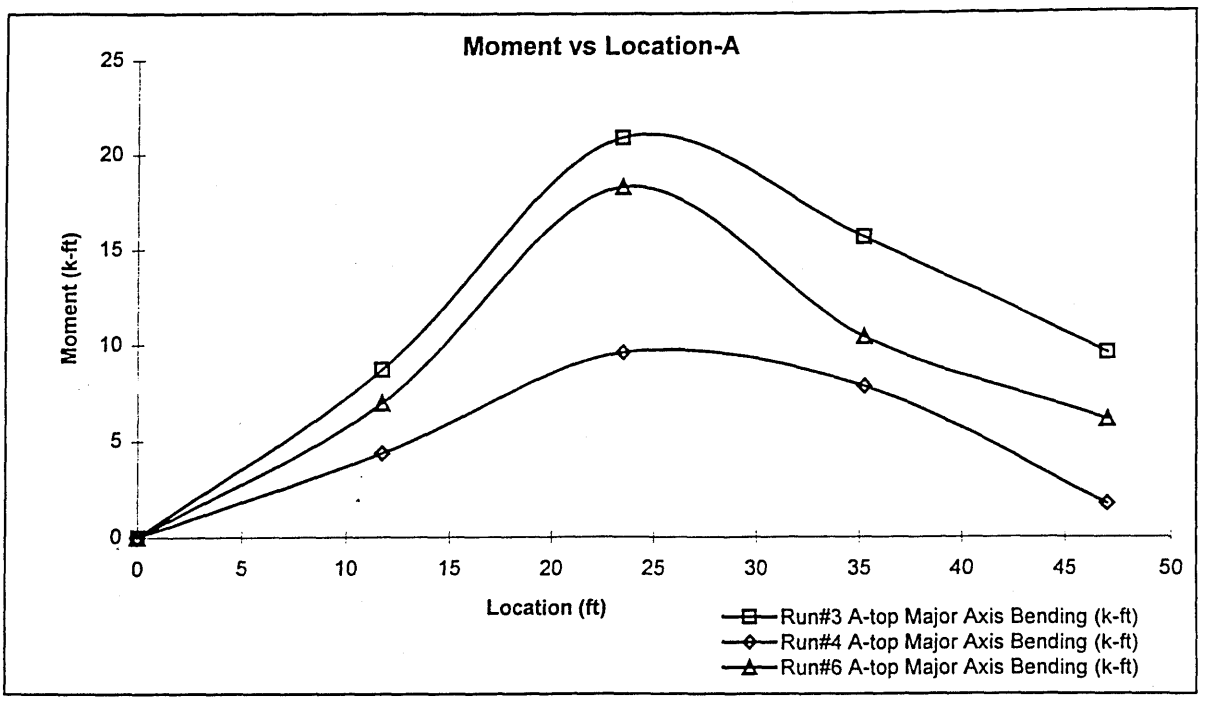

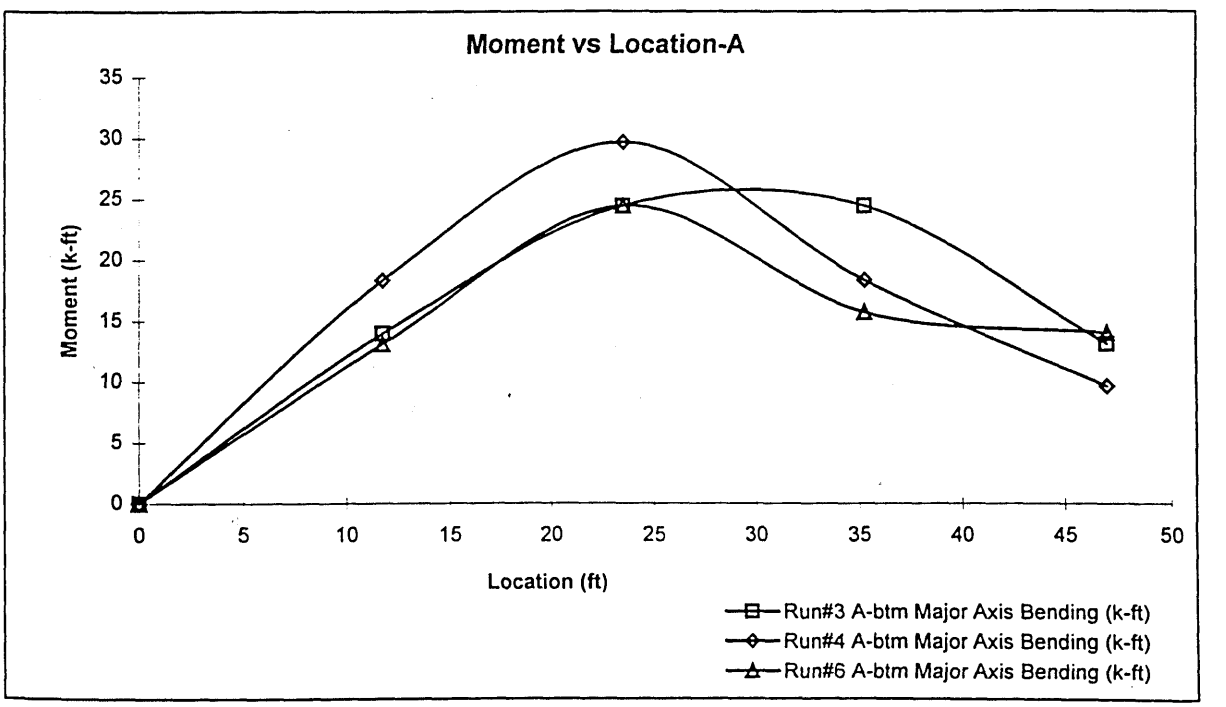

Figure 15 - Blocking Effects, Major Axis Bending - Location "A"

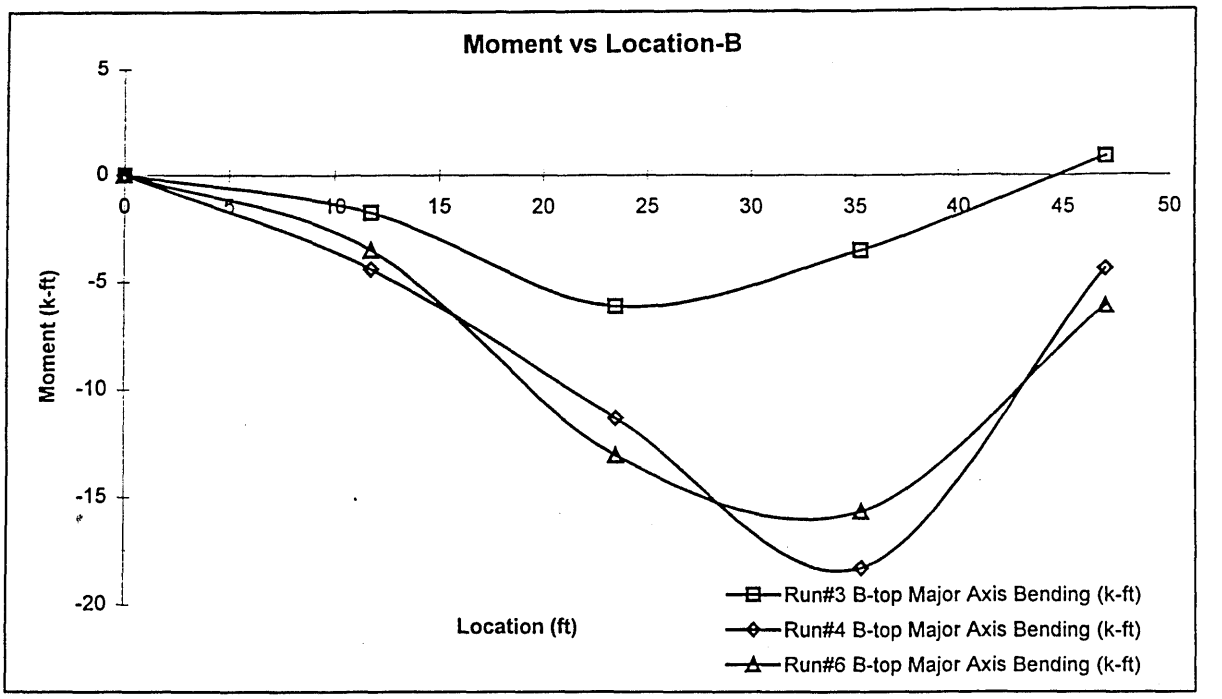

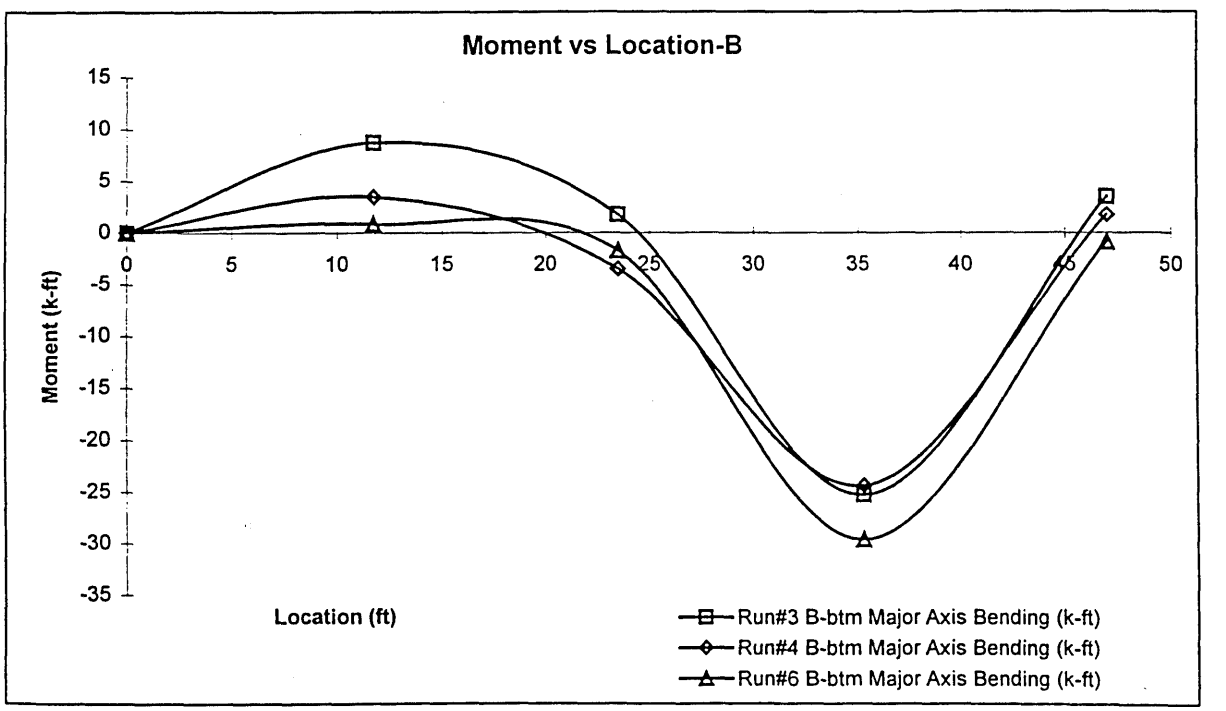

Figure 16 - Blocking Effects, Major Axis Bending - Location "B"

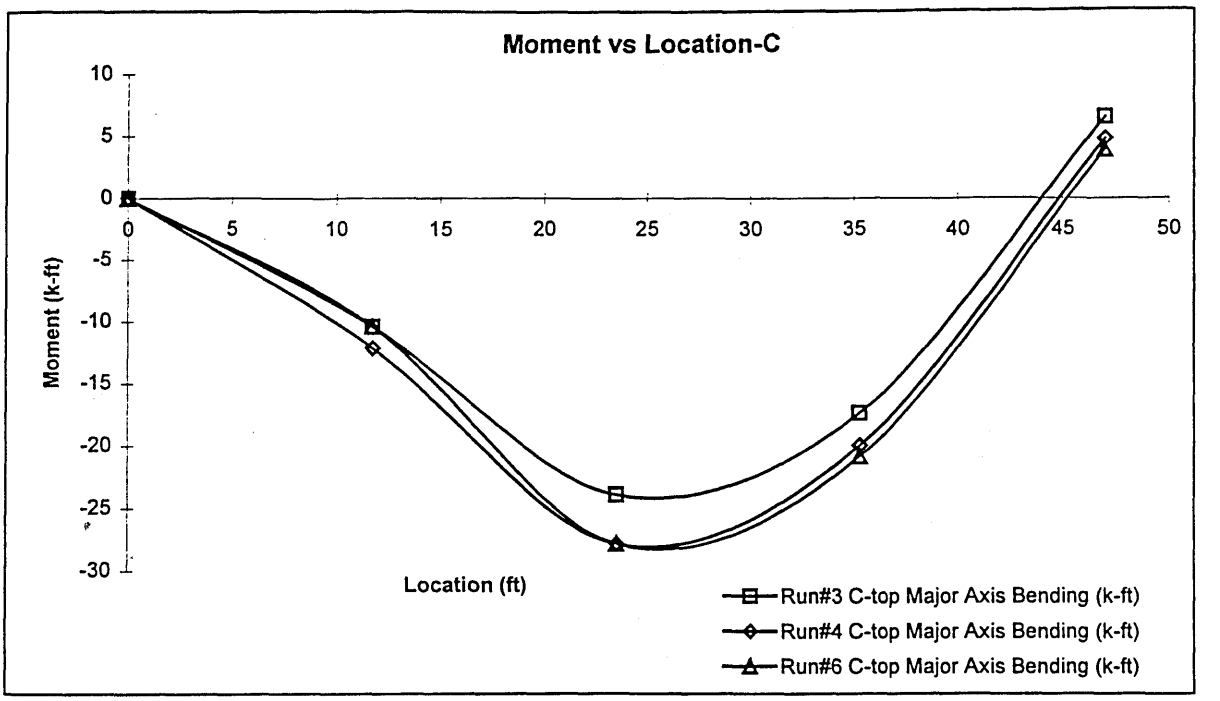

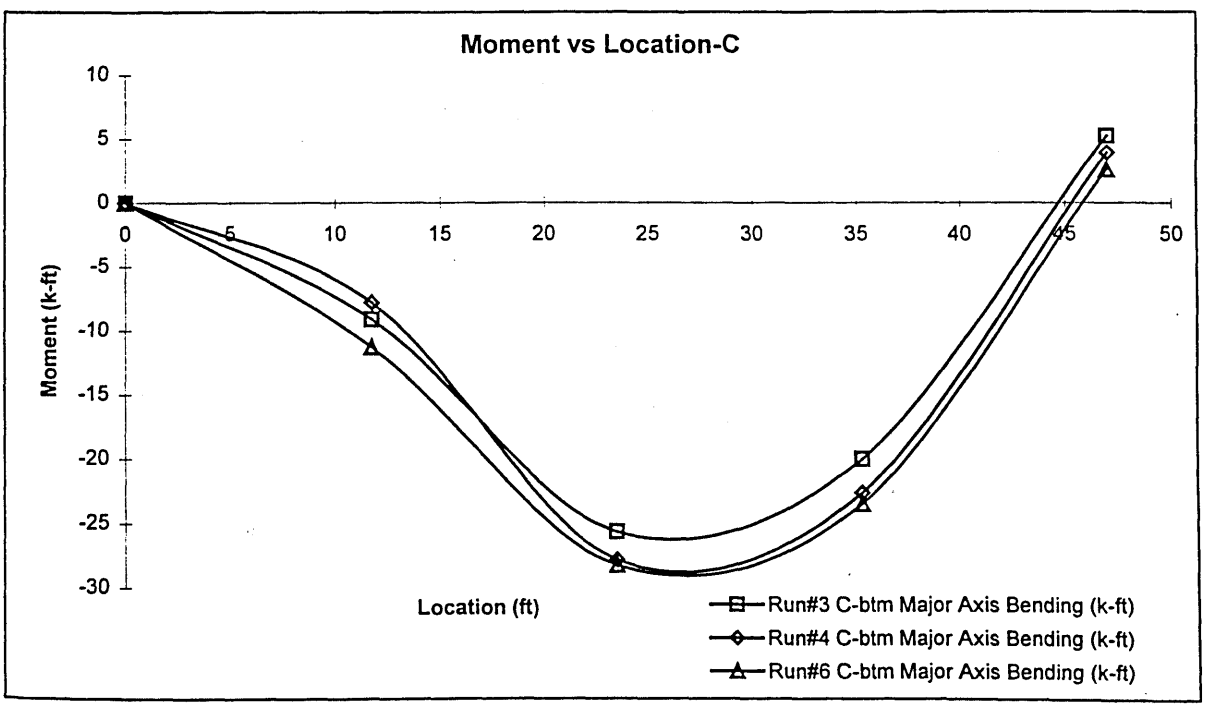

Figure 17 - Blocking Effects, Major Axis Bending - Location "C"

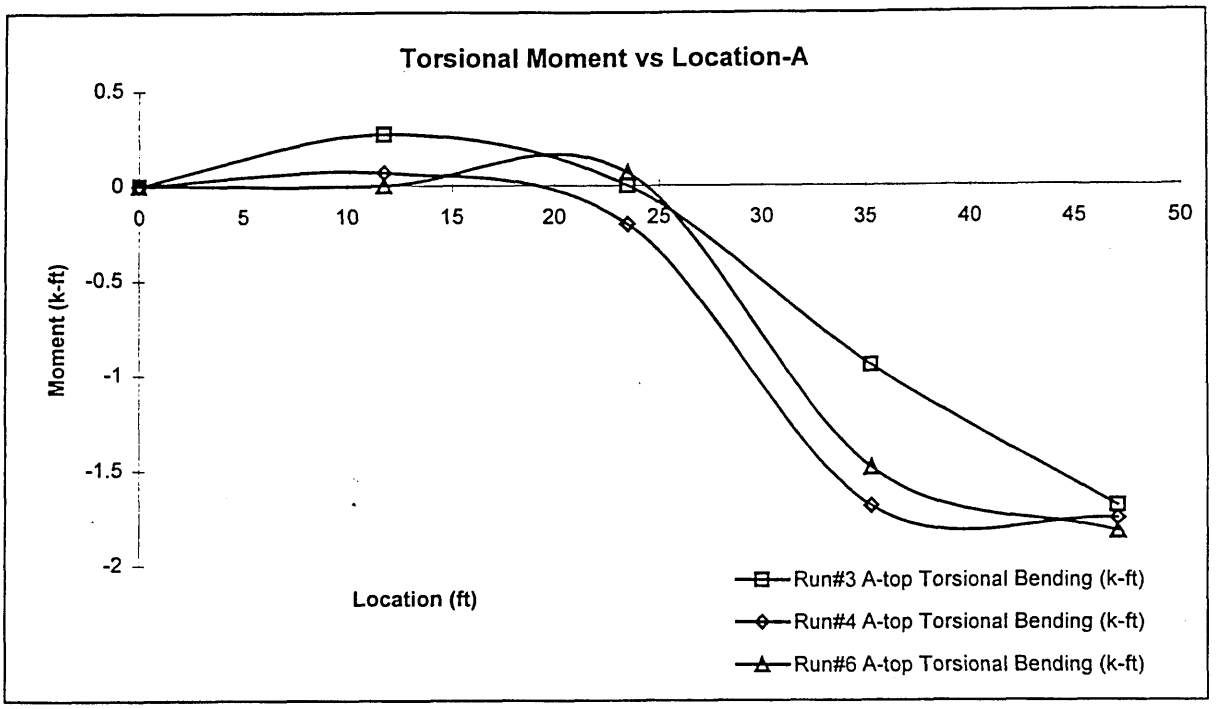

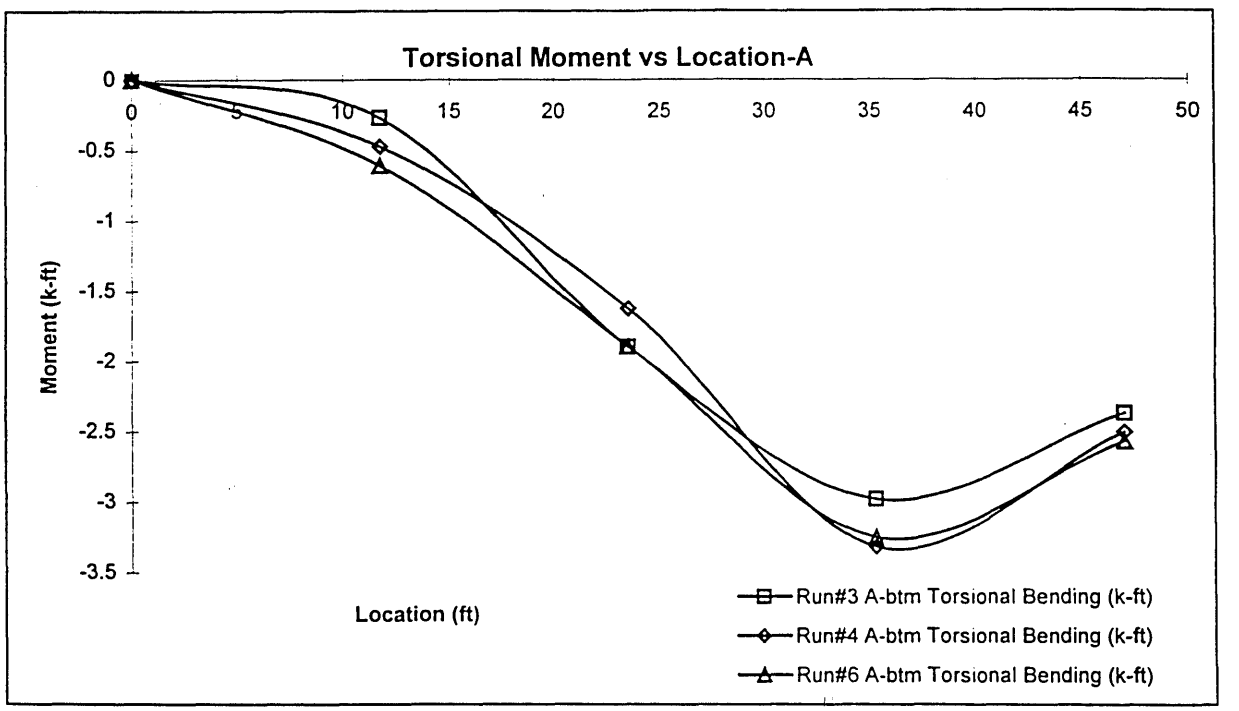

Figure 18 - Blocking Effects, Torsional Bending - Location "A"

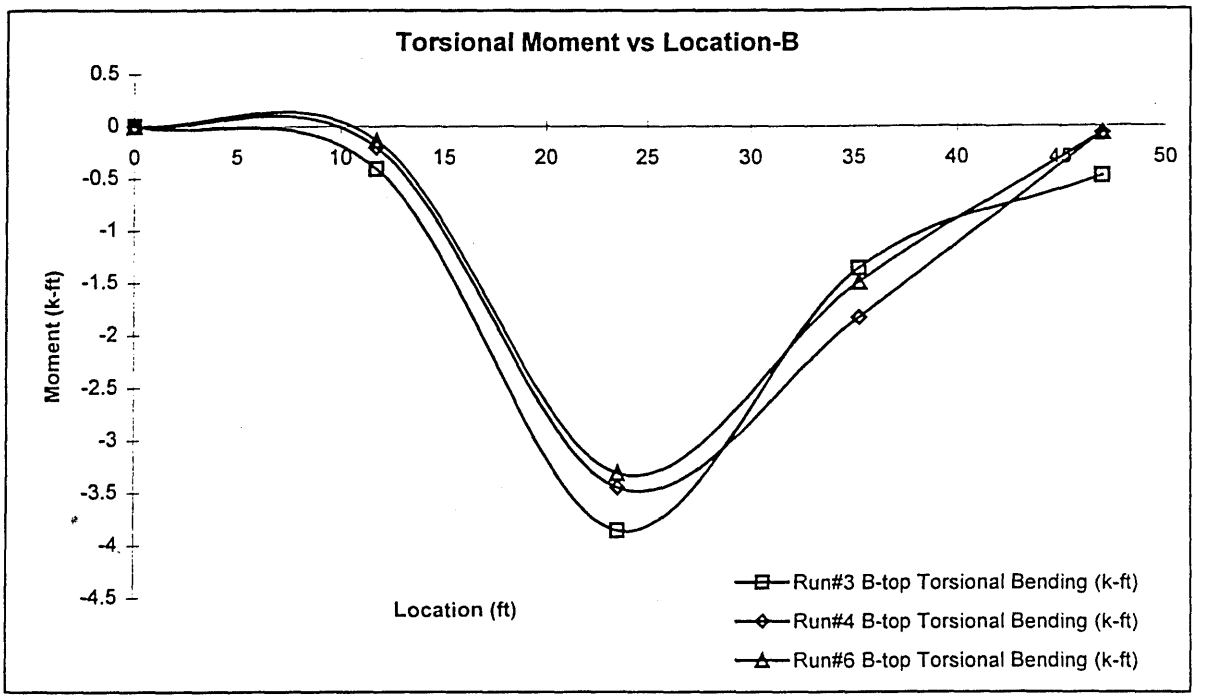

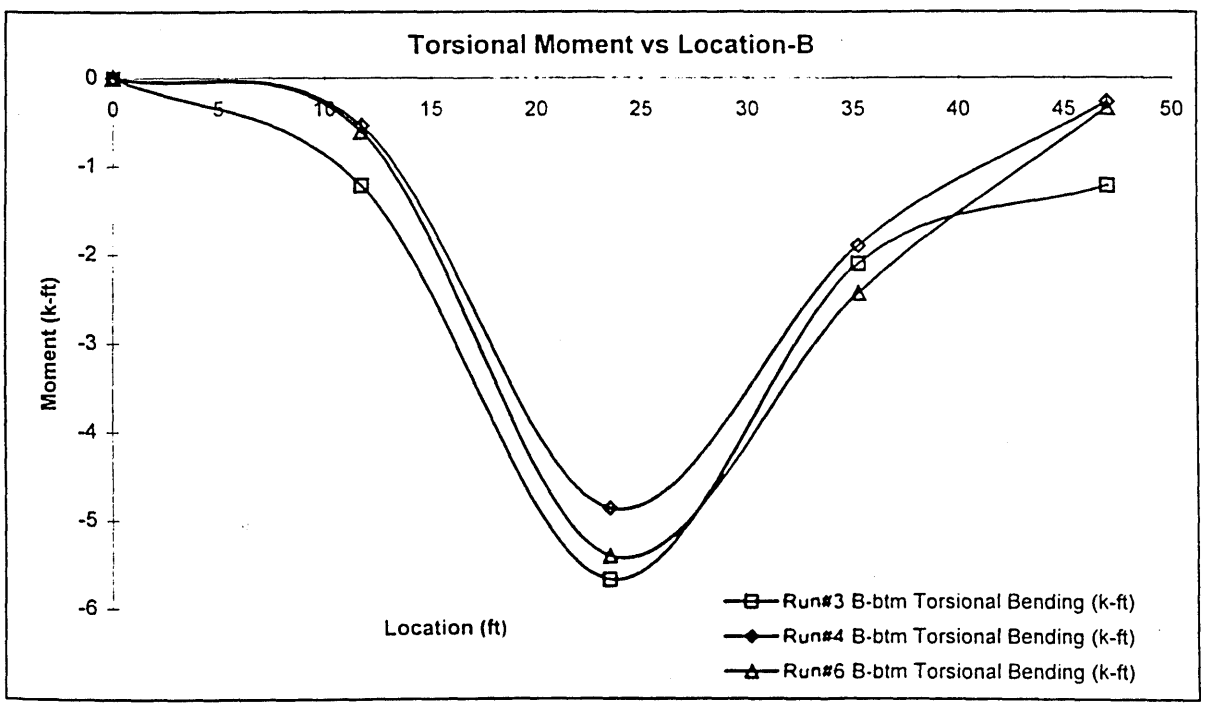

Figure 19 - Blocking Effects, Torsional Bending - Location "B"

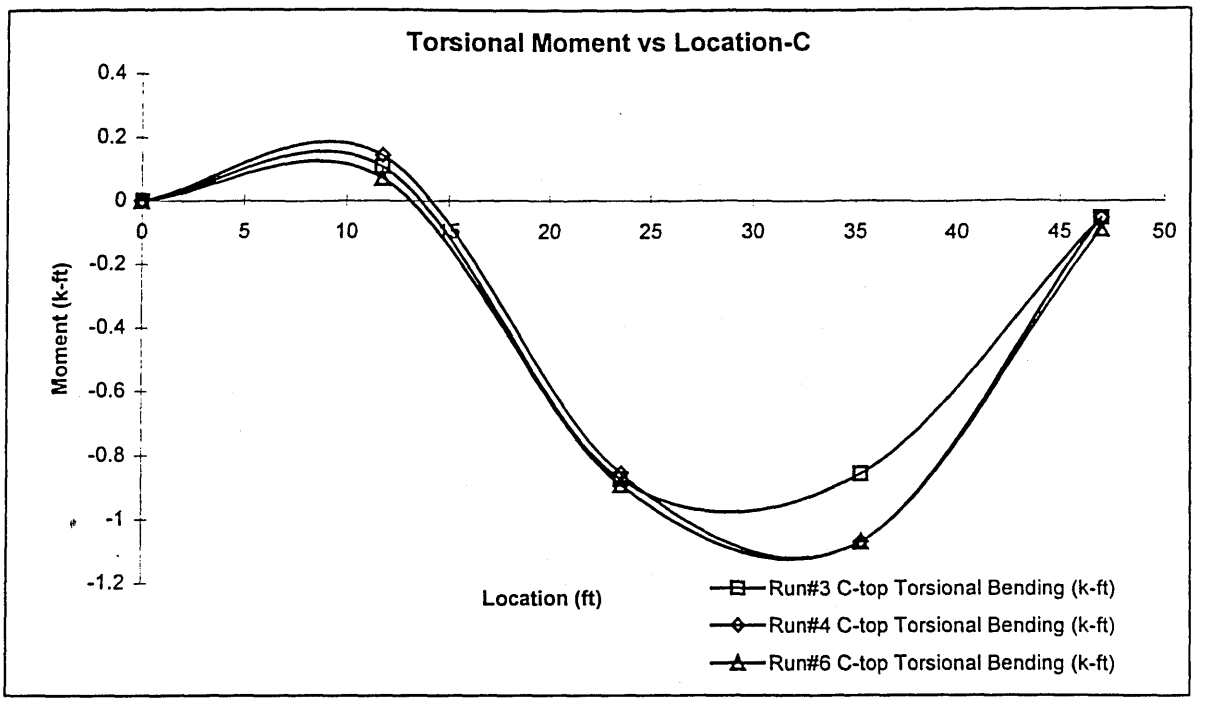

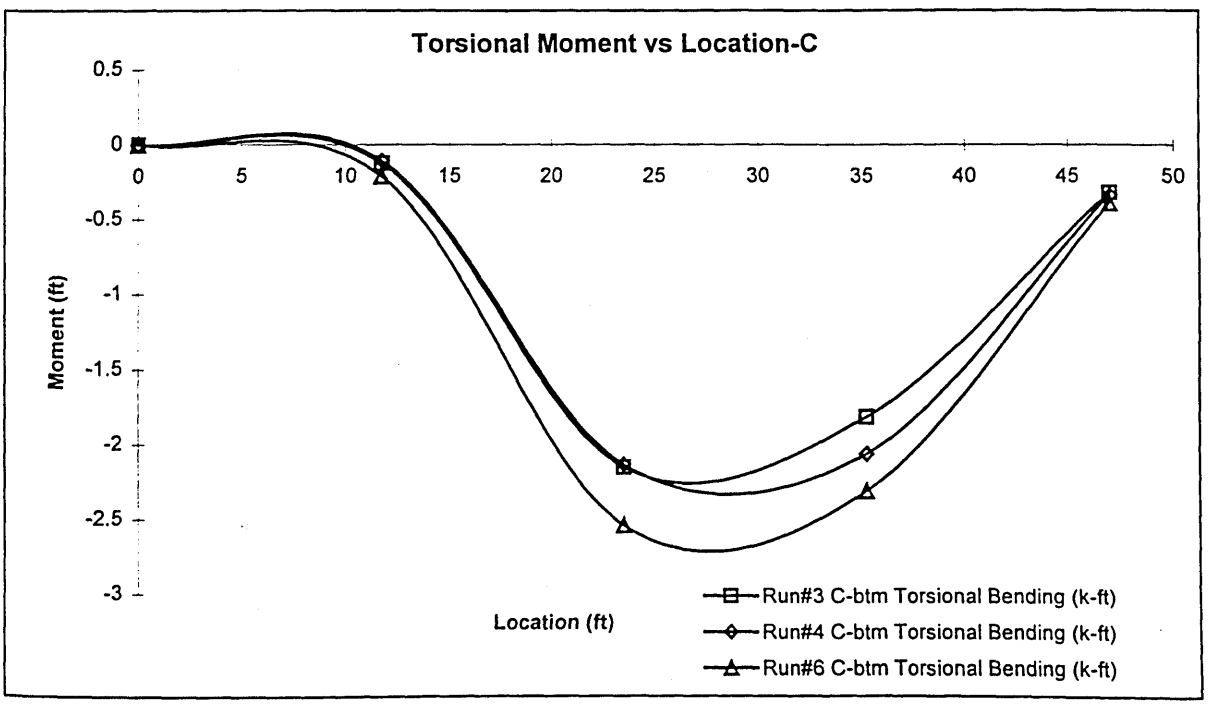

Figure 20 - Blocking Effects, Torsional Bending - Location "C"

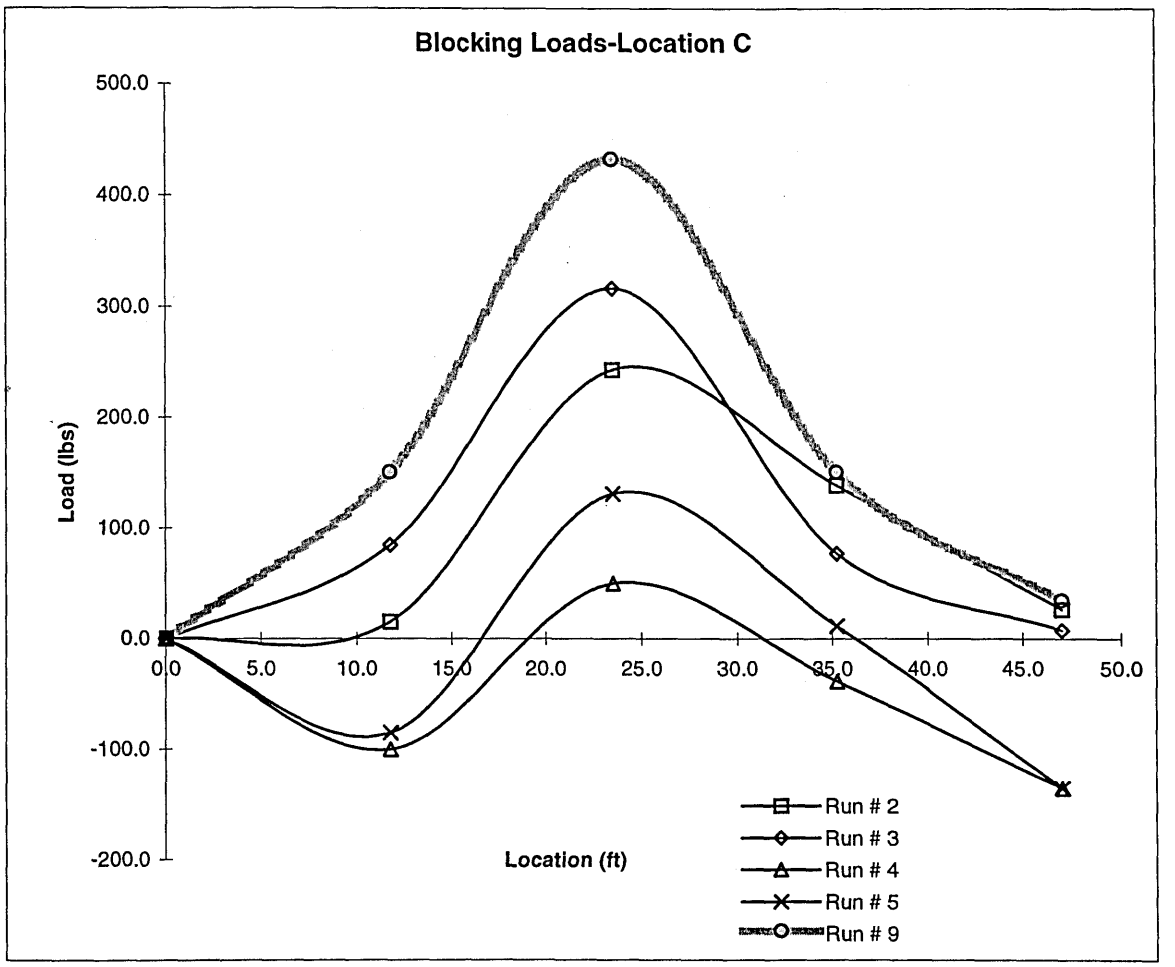

Figure 21 - Load Cell Results

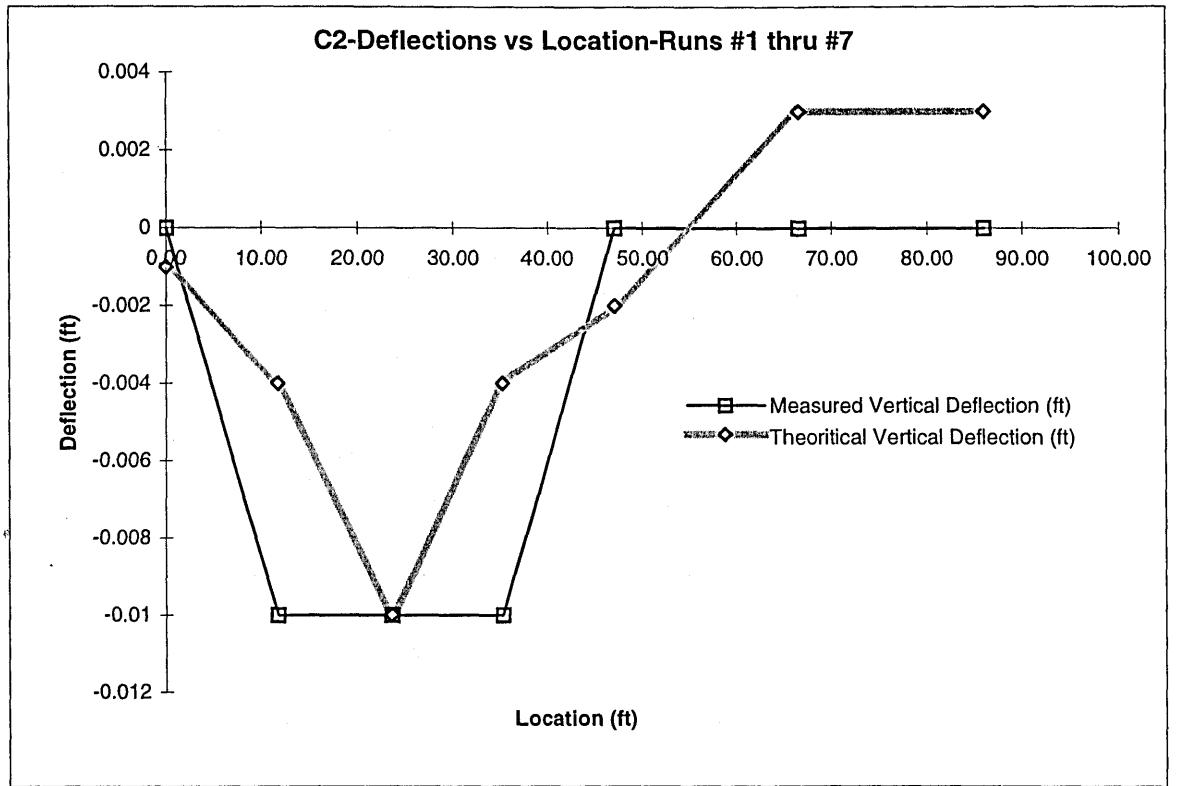

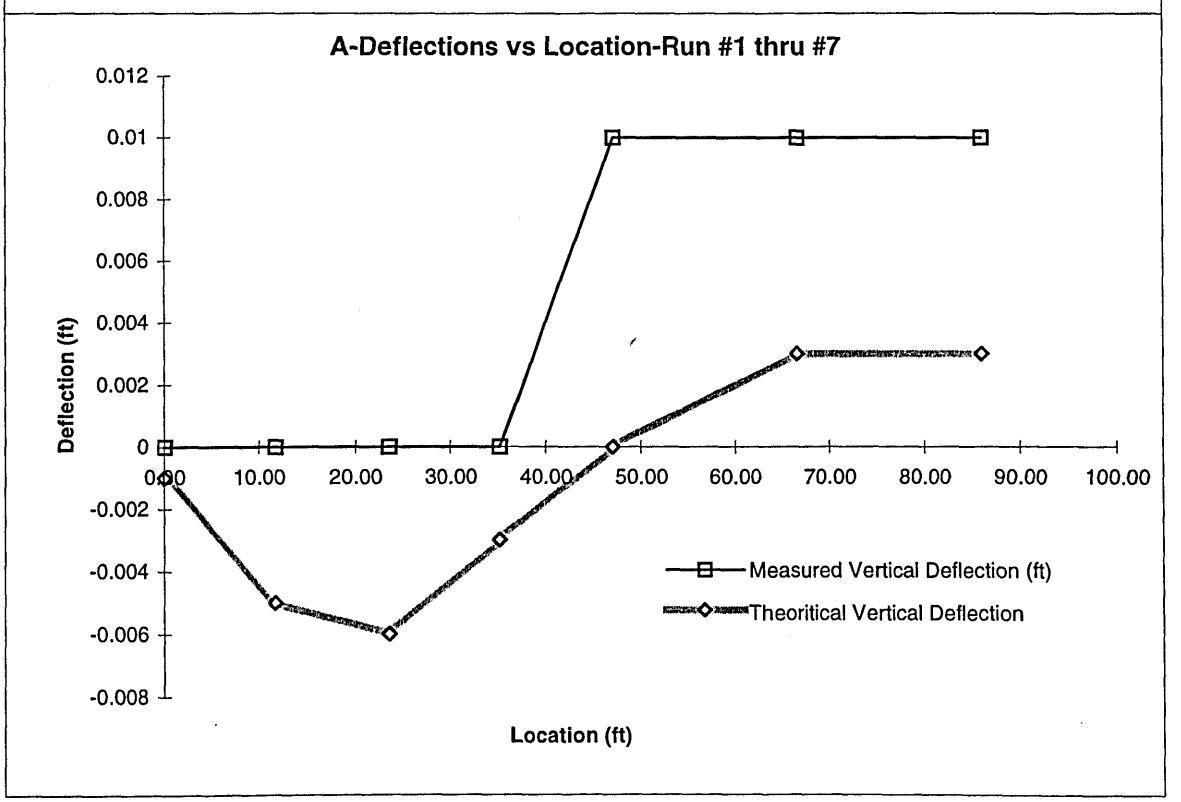

Figure 22 - Vertical Deflections

Location	Run #	Description	Measured Major Axis Bending(k-ft)	Measured Torsional Bending(k-ft)
A	3	All blocking in place	24.4	3.0
A	4	Middle blocking only	29.6	3.3
A	6	All blocking removed	24.4	3.3
B	3	All blocking in place	25.3	5.7
B	4	Middle blocking only	24.4	4.9
B	6	All blocking removed	29.6	5.4
C	3	All blocking in place	25.7	2.2
C	4	Middle blocking only	27.8	2.1
C	6	All blocking removed	28.3	2.5

Table 1 - Blocking Effects, Locations "A, B, & C"

	Measured	Multiframe	AISC	TAEG*
Maximum Moment (+)	2.3 k-ft	6.6 k-ft	12.8 k-ft	58.2 k-ft
Maximum Moment (-)	4.0 k-ft	22.6 k-ft	22.6 k-ft	62.7 k-ft

* Note: Refer to page 72, "Torsion of Exterior Girders of a Steel Girder Bridge During Concrete Deck Placement - A Design Aid" by Roddis & Kriesten, 1997

Table 2 - Comparison of Results

APPENDIX A
K-10 Report